

1. Report No. SWUTC/06/167761-1		2. Government Accession No.		3. Recipient's Catalog No.	
4. Title and Subtitle Accurate Speed Estimation Using Single Loop Detector Data		5. Report Date August 2006		6. Performing Organization Code	
		8. Performing Organization Report No. SWUTC/06/167761-1		10. Work Unit No. (TRAIS)	
7. Author(s) Yunlong Zhang, Zhirui Ye, and Yuanchang Xie		11. Contract or Grant No. 10727		13. Type of Report and Period Covered Research Final Report Sept 2005- Aug 2006	
9. Performing Organization Name and Address Texas Transportation Institute The Texas A&M University System College Station, Texas 77843-3135		14. Sponsoring Agency Code		15. Supplementary Notes Supported by general revenues from the State of Texas.	
		12. Sponsoring Agency Name and Address Southwest University Transportation Center Texas Transportation Institute The Texas A&M University System College Station, Texas 77843-3135		16. Abstract <p>Flow speed describes general traffic operation conditions on a segment of roadway. It is also used to diagnose special conditions such as congestion and incidents. Accurate speed estimation plays a critical role in a traffic management or traveler information system. Data from loop detectors has been a primary source for traffic information, and single loop detectors are the predominant source in many places. However, single loop detectors do not produce speed output.</p> <p>Several methods have been developed for speed estimation using single loop detector outputs. These methods, however, have their limitations and are often inaccurate under various traffic conditions. Some of the methods are also difficult to implement. This research project seeks to improve on the existing methods and to increase the accuracy of speed estimation. A new methodology, the Unscented Kalman Filter (UKF) method, is developed for this purpose. Datasets collected from three different freeway locations are used for speed estimation and evaluation of the proposed method. The results show that the proposed method generates accurate and stable estimations of speed. The proposed method is superior to existing methods.</p>	
17. Key Words Speed Estimation, Single Loop Detector, Unscented Kalman Filter, Large Truck Volume		18. Distribution Statement No restrictions. This document is available to the public through NTIS: National Technical Information Service 5285 Port Royal Road Springfield, Virginia 22161			
19. Security Classification.(of this report) Unclassified		20. Security Classification.(of this page) Unclassified		21. No. of Pages 74	22. Price

ACCURATE SPEED ESTIMATION USING SINGLE LOOP DETECTOR DATA

by

Yunlong Zhang
Assistant Professor
Texas A&M University

Zhirui Ye, E.I.T.
Graduate Research Assistant
Texas A&M University

and

Yuanchang Xie
Graduate Research Assistant
Texas A&M University

Research Report 167761-1

Sponsored by the
Southwest University Transportation Center
Texas Transportation Institute

October 2006

TEXAS TRANSPORTATION INSTITUTE
The Texas A&M University System
College Station, Texas 77843-3135

DISCLAIMER

The contents of this report reflect the views of the authors, who are responsible for the facts and the accuracy of the information presented herein. This document is disseminated under the sponsorship of the Department of Transportation, University Transportation Centers Program, in the interest of information exchange. Mention of trade names or commercial products does not constitute endorsement or recommendation for use.

ABSTRACT

Flow speed describes general traffic operation conditions on a segment of roadway. It is also used to diagnose special conditions such as congestion and incidents. Accurate speed estimation plays a critical role in a traffic management or traveler information system. Data from loop detectors has been a primary source for traffic information, and single loop detectors are the predominant source in many places. However, single loop detectors do not produce speed output.

Several methods have been developed for speed estimation using single loop detector outputs. These methods, however, have their limitations and are often inaccurate under various traffic conditions. Some of the methods are also difficult to implement. This research project seeks to improve on the existing methods and to increase the accuracy of speed estimation. A new methodology, the Unscented Kalman Filter (UKF) method, is developed for this purpose. Datasets collected from three different freeway locations are used for speed estimation and evaluation of the proposed method. The results show that the proposed method generates accurate and stable estimations of speed and is superior to existing methods.

EXECUTIVE SUMMARY

Single loop detectors are the most widely deployed sensors on America's highways to collect real-time vehicle data including traffic count and occupancy. However, another important traffic flow parameter, speed, can not be obtained directly from single loop outputs. For this reason, speed estimation using single loop outputs has attracted attentions from many researchers and practitioners. Several methods have been proposed for speed estimation in the past. The estimation accuracy, however, is still unsatisfactory due to several important issues. These issues include: the difficulty of accurately estimating the mean effective vehicle length; the unreasonable simplifications and assumptions for certain traffic conditions; and the drawbacks and limitations in the underlying theories of the previously proposed methods. Therefore, a methodology that can achieve accurate speed estimation using single loop data will be a very important contribution to the start-of-the-art research and can also play an important practical role in real-time traffic control and management.

This work first reviews and assesses existing speed estimation methods. These methods include the traditional g-estimator method, the log-linear regression method, the modified g-estimator method, the extended Kalman filter method, and the catastrophe theory method, etc. Three types of loop detectors used in the studies of this subject are also described and discussed.

This work then explores the subject and finds that speed estimation is a nonlinear problem. An unscented Kalman filter method is thus proposed to deal with this problem. The proposed method is analyzed and applied to real world datasets. Four datasets from three freeway locations are used for the evaluation of the proposed method. The first two datasets are collected from Peek ADR-6000 detectors; they are compiled into single loop outputs with time intervals of 30 seconds. The third dataset is collected from dual-loop detectors with time intervals of 20 seconds. The results show that the unscented Kalman filter method can generate accurate and stable estimations. Moreover, this method is not difficult to implement.

ACKNOWLEDGMENTS

The authors recognize that support for this research was provided by a grant from the U.S. Department of Transportation, University Transportation Centers Program to the Southwest Region University Transportation Center which is funded 50% with general revenue funds from the State of Texas.

TABLE OF CONTENTS

CHAPTER 1. INTRODUCTION.....	1
1.1 PROJECT OBJECTIVES.....	1
1.2 RESEARCH TASKS.....	1
1.3 REPORT ORGANIZATION	2
CHAPTER 2. LITERATURE REVIEW.....	5
2.1 TRAFFIC DETECTORS.....	5
2.1.1 SINGLE LOOP DETECTORS	6
2.1.2 DUAL-LOOP DETECTORS	7
2.1.3 PEEK ADR-6000 DETECTORS	7
2.2 SPEED ESTIMATION.....	9
2.2.1 Conventional g-Estimator Method	9
2.2.2 Log-linear Regression Method	10
2.2.3 Modified g-Estimator Methods	11
2.2.4 Extended Kalman Filter (EKF).....	12
2.2.5 Exponential Smoothing Method.....	13
2.2.6 Catastrophe Theory Method	14
2.2.7 Hybrid Model	15
2.2.8 Vehicle Signature	16
2.2.9 Other Methods	16
2.2.10 Summary.....	17
CHAPTER 3. METHODOLOGY.....	19
3.1 NONLINEAR SYSTEM OF SPEED ESTIMATION	19
3.2 THE UNSCENTED KALMAN FILTER (UKF).....	21
3.3 IMPLEMENTATION OF THE UKF ALGORITHM.....	23
CHAPTER 4. RESULTS AND DISCUSSION	25
4.1 DATA SOURCES	25
4.1.1 ADR-6000 DATA	25
4.1.2 DUAL-LOOP DATA	26
4.2 APPLICATIONS.....	27
4.3 REQUIREMENTS FOR IMPLEMENTATIONS.....	40
CHAPTER 5. ESTIAMTION OF LARGE TRUCK VOLUME	43
5.1 INTRODUCTION	43
5.2 LARGE TRUCK CLASSIFICATIONS.....	44
5.3 ESTIMATION OF LT VOLUME.....	45
5.4 APPLICATIONS.....	48
5.5 SUMMARY.....	53
CHAPTER 6. SUMMARY AND CONCLUSIONS	57
REFERENCES	59

LIST OF FIGURES

Figure 2.1 Single loop detectors.....	7
Figure 2.2 Peek ADR-6000 detectors.....	8
Figure 2.3 Transformation of occupancy to v based on empirical results.....	15
Figure 3.1 Average Vehicle Lengths over Time.....	19
Figure 3.2 Speed and the ratio of speed variance to squared speed over time.....	20
Figure 3.3 Unscented transformation of the UKF.....	22
Figure 4.1 Hourly traffic volumes on SH6 in College Station (Jan. 27, 2004).....	27
Figure 4.2 Hourly traffic volumes on IH-35 in Austin (Oct. 27, 2004).....	28
Figure 4.3 Hourly traffic volumes on IH-35 in San Antonio (Feb. 10-16, 2004).....	29
Figure 4.4 Estimated speeds by the UKF on S.H.6 (Jan. 27, 2004).....	31
Figure 4.5 Estimated speeds by the UKF on IH-35 in Austin (Lane 1, Oct. 27, 2004).....	32
Figure 4.6 Estimated speeds by the UKF on IH-35 in Austin (Lane 2, Oct. 27, 2004).....	32
Figure 4.7 Estimated speeds by the UKF on IH-35 in Austin (Lane 3, Oct. 27, 2004).....	33
Figure 4.8 Estimated speeds by the UKF on IH-35 in Austin (Lane 4, Oct. 27, 2004).....	33
Figure 4.9 Estimated speeds by the UKF on IH-35 in Austin (Lane 1, Nov. 09, 2004).....	34
Figure 4.10 Estimated speeds by the UKF on IH-35 in Austin (Lane 2, Nov. 09, 2004).....	34
Figure 4.11 Estimated speeds by the UKF on IH-35 in Austin (Lane 3, Nov. 09, 2004).....	35
Figure 4.12 Estimated speeds by the UKF on IH-35 in Austin (Lane 2, Nov. 09, 2004).....	35
Figure 4.13 Estimated speeds by UKF on IH-35 in San Antonio (Lane 1, Feb.10-16, 2003).....	36
Figure 4.14 Speed estimation under congested traffic conditions on IH-35 in Austin (Nov. 09, 2004).....	37
Figure 4.15 Estimated speeds by the EKF on IH-35 in Austin (Lane 3, Oct. 27, 2004).....	39
Figure 4.16 Sensitivity analysis of speed variance on estimation results on IH-35 in Austin (Lane 1, Oct. 27, 2004).....	41
Figure 5.1 Vehicle length distributions. a) Kernel density of vehicle lengths. b) Q-Q plot of short vehicle lengths. c) Q-Q plot of long vehicle lengths.....	46
Figure 5.2 Observed MEVL and estimated errors on S.H.6 (lane 1, Jan. 27, 2004).....	49
Figure 5.3 Observed MEVL and estimated errors on IH-35 (lane 1, Oct. 27, 2004).....	49

Figure 5.4 Observed and estimated LT volumes. a) Hourly-based LT volumes on S.H.6. b) Hourly-based LT volumes on IH-35.	50
Figure 5.5 Hourly-based traffic volumes, LT percentages and estimation errors on S.H.6. a) Traffic Volume. b) LT Percentages. c) APE.	52
Figure 5.6 Speed and LT volume estimation results for IH-35 (Nov. 9-10, 2004).	54
Figure 5. 7 IH-35 LT estimation error distribution (Nov. 9-10, 2004).....	55

LIST OF TABLES

Table 2.1 Vehicle Detector Classification	5
Table 4.1 Sample Data of ADR-6000 Outputs	26
Table 4.2 Comparison of Speed Estimation Results	38
Table 5.1 Comparison of Truck Classification Results based on “Scheme F” and LTs	45
Table 5.2 Results of hourly-based estimation of LT volume	50

CHAPTER 1. INTRODUCTION

Inductive Loop Detectors (ILDs) are the most widely deployed sensors on America's highways to collect real-time vehicle data such as traffic count, occupancy, speed, and vehicle length. Loop data can be used to actuate traffic control devices, to detect traffic congestion, incidents and so on. Such data are important for Advanced Traffic Management Systems (ATMS). Occupancy and count data are typical outputs of single loop detectors. However, another important traffic flow parameter, speed, can not be obtained directly from single loop outputs. For this reason, speed estimation using single loop outputs has attracted attentions from many researchers and practitioners.

Several methods have been proposed for speed estimation in the past. The estimation accuracy, however, is still unsatisfactory due to several important issues. The issues include: the difficulty of accurately estimating the mean effective vehicle length; the simplifications and assumptions that are not reasonable for certain traffic conditions; and the drawbacks and limitations in the underlying theories of the proposed methods. Therefore, a methodology that can achieve accurate speed estimation using single loop data will be a very important contribution to the start-of-the-art research and can also play an important practical role in real-time traffic control and management.

1.1 PROJECT OBJECTIVES

The objectives of this research project are the followings:

- 1) Review and assess the state-of-the-art related to speed estimation using single loop outputs.
- 2) Develop a methodology that can generate accurate and stable estimations of speed.

1.2 RESEARCH TASKS

The research team performed the tasks described below to satisfy the objectives stated:

- 1) State-of-the-Art Literature Review

This task involved conducting a literature review of previous works related to this research project. Papers, reports as well as other resources related to speed estimation and non-

linear system analysis were reviewed. Methods, algorithms and theories adopted in previous works were studied and evaluated.

2) Data Collection and Analysis

Data were collected from freeway traffic sensors. Loop detectors, including single and dual-loop detectors, and other detectors that utilize inductive loop technology such as Peek ADR 6000 detectors, are data sources for this research project. Data from three freeway locations provided necessary data for model development, testing, and validation.

3) Methodology Development and Implementation

After evaluating the strengths and weaknesses of previous methods in this subject, a new methodology was developed to improve speed estimation. With speed estimated by the proposed method, another algorithm was further developed to estimate large truck volume. The algorithms were coded and tested with collected sensor data.

4) Performance Evaluation

Data from multiple sources were analyzed using the proposed method and algorithm to produce speed estimations. The estimated speeds were compared with measured speeds. Also, comparisons of the proposed method and some of the previous methods were conducted. Finally, the method for the estimation of large truck volume was evaluated.

5) Final Report

The final task was the preparation of this deliverable that documents research objectives, literature review, methodology development, performance evaluation, and conclusions.

1.3 REPORT ORGANIZATION

The rest of this report is organized as follows:

- 1) **Chapter 2, Literature Review:** This chapter presents a thorough review on the methods of speed estimation developed in past studies. Three types of loop detectors are also introduced.
- 2) **Chapter 3, Methodology:** This chapter presents a new methodology to improve speed estimation.
- 3) **Chapter 4, Results and Discussion:** This chapter applies the proposed method to real world data. Results from the proposed method and other existing methods are compared and evaluated.

- 4) **Chapter 5, Estimation of Large Truck Volume:** This chapter develops an algorithm for the estimation of large truck volume, based on the results of speed estimation. The performance of large truck volume estimation is also evaluated.
- 5) **Chapter 6, Summary and Conclusions:** This chapter summarizes all the previous chapters and the findings of this study.

CHAPTER 2. LITERATURE REVIEW

This chapter provides a state-of-the-art literature review of previous works related to this research project. Loop detectors commonly used in speed estimation are introduced in the first section. These detectors include single loop detectors and dual-loop detectors. The Peek ADR-6000 detectors that provide most of the data in this study are also described. In the second section, speed estimation methods developed in previous studies are reviewed and summarized.

2.1 TRAFFIC DETECTORS

Since the first vehicle detector's installation at a Baltimore intersection in 1928, which was activated when a driver sounded his car horn at a specific location (Traffic Detector Handbook, 1991), various kinds of vehicle detectors have been developed and used for traffic control and management. Based on types of installation, traffic detectors can be broadly categorized into two classes: non-intrusive and intrusive, and the results can be further classified in terms of vehicle detection and surveillance technologies as shown in Table 2.1 (Mimbela and Lawrence, 2000; Michalopoulos and Hourdakis, 2001). Among those types of detectors, ILDs have been the most widely used vehicle detection devices for several decades in the United States because of their low costs and technology maturity.

Table 2.1 Vehicle Detector Classification

Based on Installation	Based on Technology
Intrusive	Pneumatic Road Tube
	Inductive Loop Detectors (ILDs)
	Piezoelectric Sensors
	Magnetic Sensors
	Weigh-in Motion (WIM)
Non-intrusive	Video Image Processor (VIP)
	Microwave Radar
	Infrared Sensors
	Ultrasonic Sensors
	Passive Acoustic Array Sensors

In the following subsections, three detectors adopting the inductive loop technology are discussed. In previous speed estimation studies, data from both single loop and dual-loop detectors were commonly used for experiments. Thus, this part of review will include both single and dual-loop detectors. In addition, another type of vehicle detector, the Peek ADR-6000 detectors, will also be discussed because data from them were collected and used in this research.

2.1.1 Single Loop Detectors

The evolution of the inductive loop technology can be summarized into 4 stages (Potter, 2005). From 1960's to middle 1970's, loop detector designs were based on the solid-state analog technology using discrete components (transistors, diodes, etc.). Between middle and late 1970's digital design technique was employed, which made single loop detectors capable of detecting small motorcycles and improved the overall detection reliability. From early 1980's to middle 1990's, the Metal Oxide Semiconductor—Large Scale Integration (MOS-LSI) technology significantly reduced manufacturing costs and improved reliability. Designs in this period are also called “hardware-based” designs. In the middle 1990's, the “programmable software based” digital loop detector technology was introduced. Such design significantly reduced the number of switches required in the detector by using Liquid Crystal Display (LCD).

A typical single loop system is shown in Figure 2.1 (Traffic Detector Handbook, 1991). The system consists of three components: a detector oscillator, a lead-in cable and a loop embedded in the pavement. The size and shape of loops vary largely depending on the specific application (Gordon et al., 1996). The most common loop size is 6 feet by 6 feet. When a vehicle stops on or passes over the loop, the inductance of the loop is decreased. The decreased inductance then increases the oscillation frequency and causes the electronics unit to send a pulse to the controller, indicating the presence or passage of a vehicle (Mimbela and Lawrence, 2000). Single loop detectors output occupancy and vehicle count data every time interval (20 sec, 30 sec, etc.).

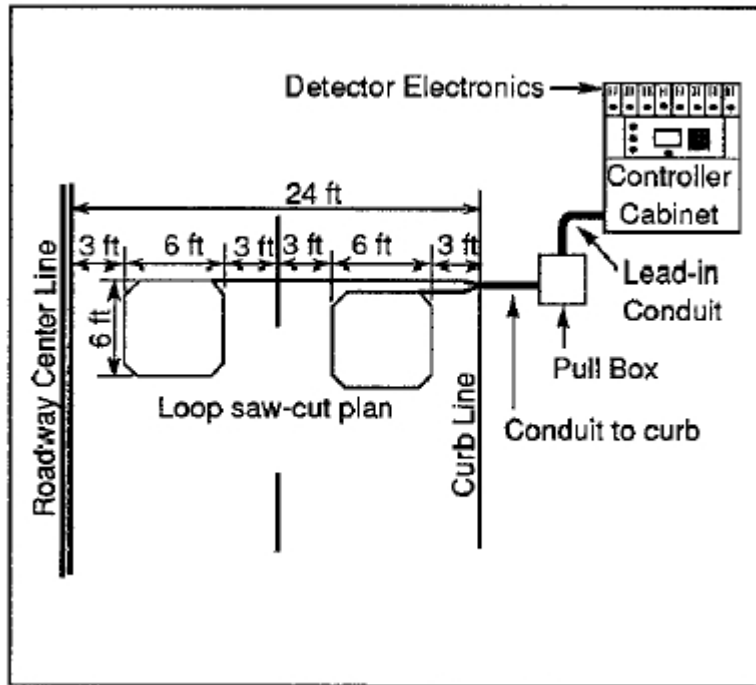


Figure 2.1 Single loop detectors.

2.1.2 Dual-loop Detectors

Dual-loop detectors are also called speed traps, T loops, or double-loop detectors. In a dual-loop system, two consecutive single inductance loops, called “M loop” and “S loop”, are embedded a few feet apart. With such a design, when one of them detects a vehicle, a timer is started in the dual-loop system and runs until the same vehicle is detected by the other loop. Thus, in addition to outputs of vehicle count and occupancy data, individual vehicle speeds can be trapped through the dividend of the distance between those two single loops by the elapsed time (Nihan, 2002). Dual-loop detectors can also be used to measure vehicle lengths with extra data extracted from controllers’ records (Coifman and Cassidy, 2002).

2.1.3 Peek ADR-6000 Detectors

A Peek ADR-6000 detector is also known as an *Idris* or *Smart Loop system*. The ADR-6000 detector uses state-of-the-art inductive loop technology and patented Idris technology (Peek Traffic, 2004). Idris is an automatic vehicle detection and classification technology. ADR-6000

detectors are installed under pavement, as shown in Figure 2.2. In each lane, there are two single loops placed apart with a vehicle axle detector in the middle. Axle detectors consist of smaller loops.

Different from the single and dual-loop detectors, the ADR-6000 detectors detect and output data for each vehicle including vehicle speed, vehicle length, vehicle classification, and presence time. Individual vehicle speeds are trapped by vehicle signatures generated in the system. Each vehicle passing over the inductive loop will generate a specific shape of signature containing a leading and trailing edge. Thus, each vehicle will have two signatures after passing the detector. The vehicle speed can be trapped by matching two points from these two signatures. Based on individual vehicle presence time, the occupancy during a time interval can be easily calculated. Thus, such detectors are able to provide traffic count and occupancy data, which are typical outputs of single loop detectors.

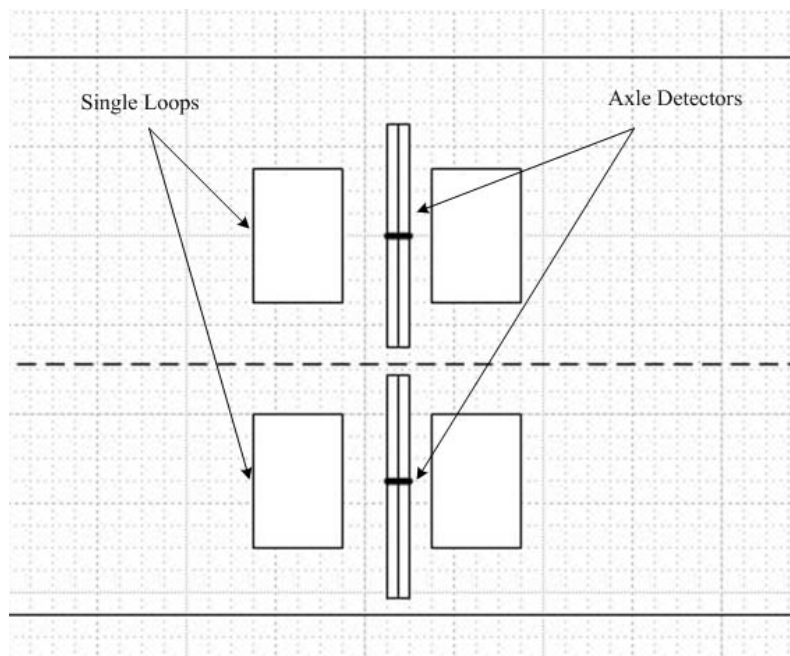


Figure 2.2 Peek ADR-6000 detectors.

2.2 SPEED ESTIMATION

With the wide deployment of the single loop detectors, plus the unavailability of speed data directly from such detectors, a variety of speed estimation methods have been developed using single loop outputs. This part of review presented below focuses on the discussion of speed estimation methods in the literature.

2.2.1 Conventional g -Estimator Method

The first method of speed estimation, the conventional g -estimator method, was proposed by Athol (Athol, 1965). Base on the definition of occupancy, the author presented the interrelationship between operational traffic flow characteristics, which is shown in Equation (2.1).

$$\bar{s}_k = \frac{1}{g} \times \frac{N_k}{T \times O_k} \quad (2.1)$$

where

k = time interval index;

\bar{s}_k = average speed (space mean speed) during k th time interval (miles per hour);

T = duration of time intervals (second);

N_k = vehicle count during k th time interval (vehicles per time interval per lane); and

g = an estimator incorporating site characteristics of average vehicle length and single loop length.

In the calculation of this method, g is an estimate of the reciprocal of Mean Effective Vehicle Length (MEVL), which is denoted as \bar{L} and is equal to the sum of the average vehicle length (\bar{l}) and the single loop length. In practice, g is set to a constant value. For instance, the Chicago Traffic System Center (TSC) uses 1.9 as the constant g value (McDermott, 1980), and the Washington State Department of Transportation (WSDOT) uses $g = 2.4$ with $T = 300$ seconds (Ishimaru and Hallenbeck, 1999).

The study of WSDOT showed that this constant g -estimator method did not provide satisfactory estimation accuracies. Actually, the interrelationship shown in Equation (2.1) is based on two assumptions: 1) vehicle lengths are constant during each time interval; and 2)

traffic is uniform (e.g., vehicles have the same speed and the spacing between vehicles is constant). However, as pointed out by Hall and Persuad (1989), those assumptions may not be valid under certain traffic conditions. In reality, the effective vehicle length (\bar{l}) may have large variations with the presence of long vehicles, such as commercial trucks. Moreover, vehicles on freeways are not steered at a same speed; speed variance sometimes becomes a significant factor due to congestion or other conditions and thus should not be ignored.

2.2.2 Log-linear Regression Method

To account for the variation of vehicle lengths, a dynamic g -estimator method was developed. Wang and Nihan (2000) calculated the g value for each time interval as a function of the MEVL (\bar{l}). The relationship of occupancy, count, average vehicle length, and speed is developed by Dailey (1999) and denoted in Equation 2.2.

$$\frac{E_k(O_k)}{N_k} = \frac{\bar{l}_k}{T} \left[\frac{\sigma_k^2}{\bar{s}_k^3} + \bar{s}_k^{-2} \right] \quad (2.2)$$

where

$E_k(O_k)$ = expectation of occupancy measurement at k th time interval, equaling to O_k for perfect measurement

N_k = count measurement at k th time interval

\bar{s}_k^2 = average speed at k th time interval

\bar{l}_k = mean effective vehicle length at k th time interval

σ_k^2 = speed variance at k th time interval

T = duration of the time interval

Wang and Nihan (2000) also conducted a study on the ratio of σ_k^2 / \bar{s}_k^2 and found that values were very low. Consequently they assumed that speed variance can be ignored, and the following equation was then derived after statistical transformations:

$$\bar{l}_k^2 = \frac{E^2(O_k) \times \sigma_{lk}^2}{V(O_k)} \quad (2.3)$$

where σ_{lk}^2 is the variance of vehicle lengths at k th time interval, and $V(O_k)$ is the occupancy variance. After introducing some additional variables, such as a high-flow dummy, to account for σ_{lk}^2 , a regression model of the MEVL at k th time interval was established and is shown in Equation (2.4).

$$\ln(\bar{L}_k) = \beta_0 + \beta_1[2\ln(E(O_k)) - \ln(V(O_k))] + \beta_2 \times \ln(N_k) + \beta_3 \times HFD + \beta_4 \times LFD + \varepsilon_k \quad (2.4)$$

where HFD is a high-flow dummy, LFD is a low-flow dummy, β s are coefficients, and ε_k is a white noise.

However, our experiments showed that the correlation coefficient of the regression model might be very low due to the variations of speed and effective vehicle length. In addition, ignoring speed variance may lead to certain level of inaccuracy.

2.2.3 Modified g-Estimator Methods

In order to reduce the influences of long vehicles and congested traffic conditions, two studies (Coifman, 2003; Lin et al., 2004) modified the g -estimator method. They used median values of speed and vehicle passage time respectively, instead of mean values adopted in the g -estimator method. The modified median g -estimator methods can reduce the skewnesses of the distributions of speed and pace (the reciprocal of speed). However, additional problems arise with the modified g -estimator methods. In the study by Coifman (2003), to estimate the median speed in a single lane, the time unit (length of time intervals) of speed estimation should be long enough (e.g., 5 minutes) to ensure that sufficient sample size (number of vehicles) is achieved according to the sampling criteria. Thus, to obtain good estimates of speed for short time units such as 30 seconds, it is required to combine vehicle data across several lanes. But in doing this, it is impossible to identify speed difference across single lanes. This is because different lanes at a location tend to show different temporal patterns of speed in reality, especially when there exist large differences of traffic flow between lanes.

In the other study (Lin et al., 2004), the median vehicle passage time (l_{median} / s_{median}) at each time interval is used to replace the mean vehicle passage time (l_{mean} / s_{mean}), and the median vehicle passage time is approximated by $(l/s)_{median}$. To implement this method, the information

of passage times ($Time_1$ when the vehicle reaches the front part of the loop and $Time_2$ when the rear end of the vehicle leaves the single loop) is required from each vehicle so that the value of $(l/s)_{median} = (Time_2 - Time_1)_{median}$ can be obtained. However, the common outputs (vehicle count and occupancy) of single loops do not include such information.

2.2.4 Extended Kalman Filter (EKF)

Dailey (1999) presented a statistical method, the Extended Kalman Filter (EKF) method, to linearize the measurement equation for speed estimation. A general Kalman Filter (KF) model includes two equations, a state-transition equation and a measurement equation (Bozic, 1994). These two equations are

$$x_k = A\bar{x}_{k-1} + Bu_{k-1} + v_{k-1} \quad (2.5)$$

$$y_k = Hx_k + n_k \quad (2.6)$$

where

x_k = predicted value at k th time interval from previous time interval

y_k = measurement at k th time interval

u_{k-1} = control input

v_k = process noise

n_k = measurement noise

The KF method operates with two phases per time interval: time update phase to “predict” new state, and measurement update phase to “correct” new state. In a speed estimation application, average speed at k th time interval is the state, and occupancy over count ratio, which can be gathered from single loop detectors, is the measurement. The EKF linearizes the measurement equation, which is established based on Equation (2.2) and assumes perfect measurement of occupancy data.

However, there are several issues in the EKF and its speed estimation implementation. As pointed out by Julier et al. (Julier and Uhlmann, 1997), linearization in the EKF will produce highly unstable filters if assumptions are not met, and the derivation of the Jacobian matrices often lead to significant implementation difficulties. Note that in the EKF, Jacobian matrices are

partial derivatives of a nonlinear function with respect to its variables. To better describe the drawbacks of the EKF, we assume x is a random variable and $y = f(x)$, then the mean value of y can be achieved by expecting $f(x)$, this can be shown as

$$\bar{y} = E[y] = E[f(x)] \quad (2.7)$$

Only for linear Gaussian system, we can get $\bar{y} = f(\bar{x})$; for nonlinear systems, this is not the case. While in the EKF, the mean value is calculated as $\bar{y} = f(\bar{x})$, not $\bar{y} = E[f(x)]$. The EKF only considers the first order of Taylor series (Equation 2.8) to perform linearization.

$$f(x_{k-1}) = f(x_{k-1}^a) + f'(x_{k-1}^a)(x_{k-1} - x_{k-1}^a) \quad (2.8)$$

In the implementation of the EKF, the state variable (average speed) is calculated based on the two previous states using a state transition matrix

$$G = \begin{pmatrix} a & b \\ 1 & 0 \end{pmatrix} \quad (2.9)$$

Coefficients a and b represent weights for the two previous states. In the EKF method, these two coefficients are derived using Auto Regression (AR) method with 2 orders based on measured speed data. Theoretically, the accuracy of filtering results largely depends on the number of orders, and the coefficients of AR have a great effect on the results. Since experimentally measured speed data can only represent the variation of some speed change patterns in certain time duration, such AR coefficients may not always lead to good estimation accuracy.

2.2.5 Exponential Smoothing Method

Hellinga (2002) used a volume weighted exponential smoothing method to improve the traditional g-estimator method. This method is applicable to freeway TMS that contains both single and double loop detector stations. Thus, MEVL measured from dual-loop detectors can be applied to single loop detectors nearby. However, it is found that the correlation between the MEVLs measured from two detectors in a detector station set is very low, which is caused by sampling error. To decrease sampling error, it is needed to choose a longer time period, while this is difficult to do in practice. Therefore, the exponential smoothing method is proposed to avoid the problem of having to select a fixed sampling period duration.

Estimated results using this method are approximately 20% more accurate than the traditional g-estimator method, while estimation errors are still relative high as shown in the study. In addition, the applicability of this method is limited since this method is not applicable when there are no double loop detectors presented in the vicinity of single loop detectors.

2.2.6 Catastrophe Theory Method

The Catastrophe Theory was originated by French mathematician Rene Thom in the 1960's and developed by Zeeman (1977). Catastrophe means the loss of stability in a dynamic system. As a special branch of dynamical system theory, the Catastrophe theory studies and classifies phenomena characterized by sudden shifts in behavior arising from small changes in circumstances. This theory was used by Hall (1987) and Pushkar (1994) to estimate speed using single loop outputs. The authors established a relationship between traffic variables (occupancy, speed, etc.) and a 3-dimensional folded surface in the Catastrophe Theory. The Catastrophe Theory model is presented in Equation (2.10).

$$4x^3 + 2ux + v = 0 \quad (2.10)$$

where x is the state variable associated with speed, and u, v are control variables related to flow and occupancy respectively. To model traffic flow behavior and estimate speed, the author used two simple linear transformations, as shown in the following, to establish the relationship between x and speed as well as u and flow.

$$\begin{aligned} x &= \text{speed} - \text{speed_at_capacity} \\ u &= (\text{flow} - \text{capacity}) / 1000 \end{aligned}$$

The transformation between v and occupancy is accomplished in *ad hoc* manner and is shown in Figure 2.3 (Hall, 1987). When occupancy and flow data are available, speed can be estimated using the Catastrophe Theory model and those three transformations. Although those transformations simplify the speed estimation, the involvements of empirical data and results (i.e., capacity, speed at capacity, and arbitrary relationship between v and occupancy) may introduce significant errors.

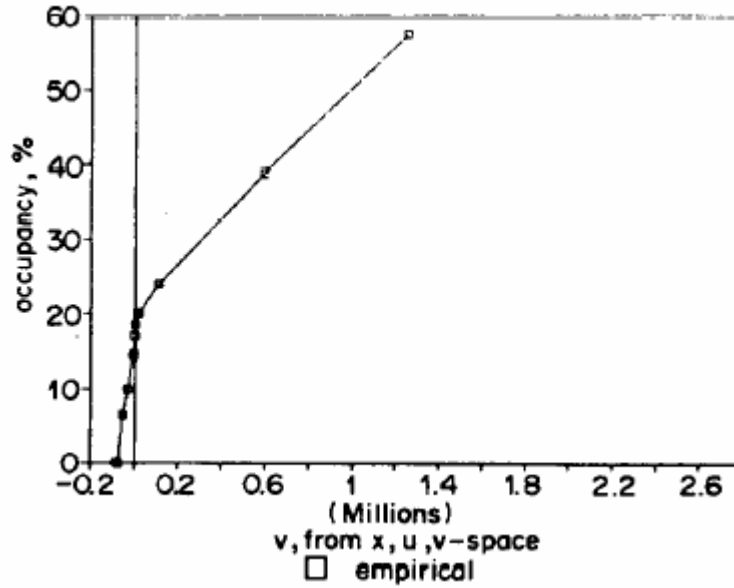


Figure 2.3 Transformation of occupancy to v based on empirical results.

2.2.7 Hybrid Model

Yao et al. (2004) presented a hybrid model, which consists of two sub-models for speed estimation under both free flow and traffic congested conditions. The hybrid model is

$$\begin{aligned} \bar{s}_k &= s_f e^{-O_k} & O_k &\leq O_{threshold} \\ \bar{s}_k &= s_m \ln(1/O_k) & O_k &\geq O_{threshold} \end{aligned} \quad (2.11)$$

where s_f and s_m represent speed under free flow and congested flow conditions respectively. s_f can be estimated by using single loop data and dropping out congested data. A constant MEVL is also needed to calculate s_f . With s_f obtained, s_m is empirically calculated by $s_m = s_f / e$. A threshold occupancy value $O_{threshold}$ is used to identify whether traffic flow is free or congested.

This method is simple once the initial parameters (e.g., s_f , s_m , $O_{threshold}$, \bar{L} , etc) are calibrated. However, the constant s_m may contribute to large errors because traffic flow and speed is rather unstable under congested conditions. The authors do not provide a sensitive analysis of s_m . Moreover, the threshold value $O_{threshold}$ varies, especially under different weather conditions.

2.2.8 Vehicle Signature

As part of traffic monitoring and surveillance systems, sensor technology has been receiving a lot of attentions and many detectors have been developed to obtain more comprehensive and accurate traffic data. In the middle of 1990's, the "programmable software based" digital loop detector technology was used to upgrade existing "hardware-based" designs, by replacing a very few switches with an active LCD (Potter, 2005). With such a design, more information can be obtained from ILDs besides occupancy and vehicle count data. An ILD system with high speed scanning detector cards is able to capture the "inductive signatures" of different types of vehicles. Each vehicle passing over the inductive loop will generate a different shape of signature containing a leading and trailing edge. The signature information has been used in speed estimation. Sun and Ritchie (1999) proposed a new speed estimation technique using single ILD signatures, with signal processing and linear regression techniques. A simple linear regression model is presented to model the relationship between speed and slew rate. Slew rate is the edges (either leading or trailing) that represent the rate of metallic mass of vehicle passing over the loop magnetic field. Oh et al. (2002) estimated speeds using vehicle signatures through extracting signature feature vectors.

The vehicle signature method is different from the previous methods in that different information (vehicle signature) is used for speed estimation. Note that in this research, except for the vehicle signature method, other speed estimation methods all use count and occupancy data from loop detectors.

2.2.9 Other Methods

Several other methods were also proposed in previous works. They are included in this part of review as those methods are difficult to be classified and given appropriate names. Coifman (2001) stated that under free flow conditions, occupancies from loop detectors are low. Thus, a threshold value of occupancy was set to identify free flow traffic with a specific free flow speed. This method improves the vehicle length estimates under free flow conditions assuming a linear relationship of MEVL, speed, occupancy and count.

Some other studies have tried to estimate speed by exploring the relationship between speed and occupancy. For instance, An Istanbul study (Ogut, 2004) used data from four locations

to analyze and establish a regression model between speed and occupancy, in which occupancy was a function of speed. This method does not take vehicle length and other factors into account.

2.2.10 Summary

From the above reviews, several issues exist in speed estimation using single loop outputs. First of all, it is difficult to accurately estimate the MEVL for each time interval. A common MEVL is generally used in practice. Moreover, a simplified linear relationship between speed and other parameters are usually used in past studies. Such simplifications will produce estimation errors. Finally, previous methods have their own drawbacks in underlying theories. As a result of these issues, the accuracy of estimation results is generally unsatisfactory.

CHAPTER 3. METHODOLOGY

3.1 NONLINEAR SYSTEM OF SPEED ESTIMATION

As mentioned earlier, the problem of speed estimation is a nonlinear system as shown in Equation 2.2. In this system, the MEVL (\bar{L}_k) and the speed variance (σ_k^2) are major variables contributing to the nonlinearity. At a given location, \bar{L}_k varies over time and its variation is mainly determined by the involvement of trucks and other long vehicles. This variable, however, is hard to estimate accurately. Thus, a common value \bar{L} is usually used during estimation. Figure 3.1 shows an example of average vehicle lengths varying over time from 5 a.m. to midnight, using real world data. In this figure, the time interval is 30 seconds. It can be seen that average vehicle lengths during nighttime are generally larger than those during daytime, while the figure does not show any clear pattern of the average vehicle length over time.

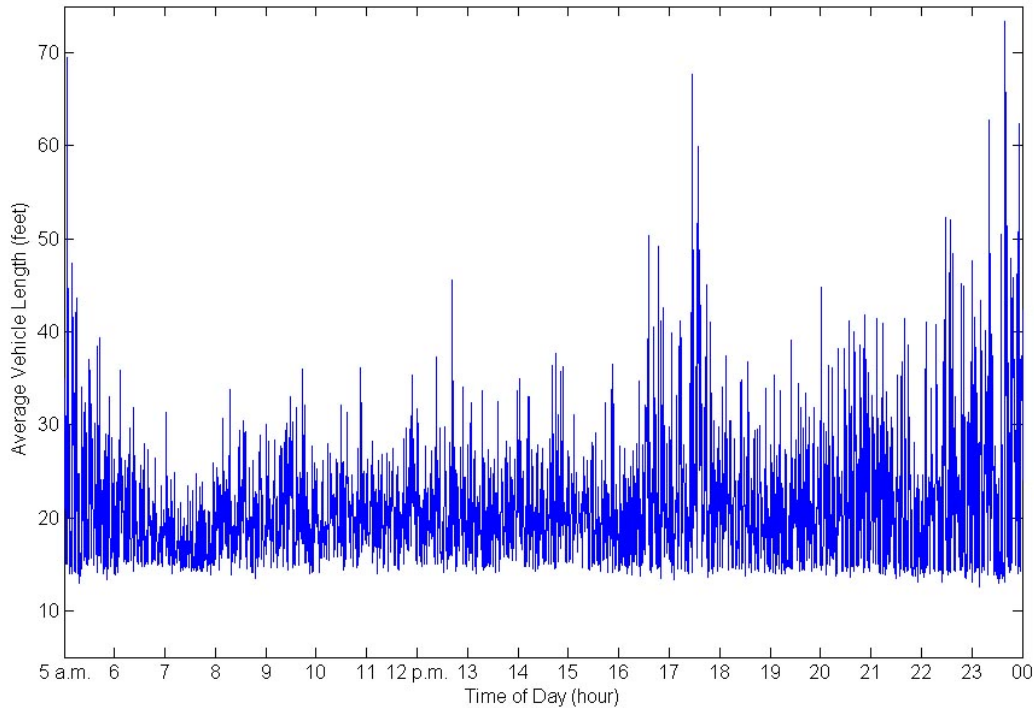


Figure 3.1 Average vehicle lengths over time.

The effect of speed variance (σ_k^2) on the nonlinearity of the speed estimation system was not explored in past studies. This is because outputs from either single loop or dual-loop detectors do not provide individual vehicle speed information. Peek ADR-6000 detectors make it possible to analyze the influence of speed variance. Real-world data from ADR-6000 detectors can be compiled to calculate the ratio of speed variance over squared speed (σ_k^2 / \bar{s}_k^2). An example of this ratio over time is shown in Figure 3.2, which also displays speed \bar{s}_k over time (5 a.m. to midnight) in its upper portion.

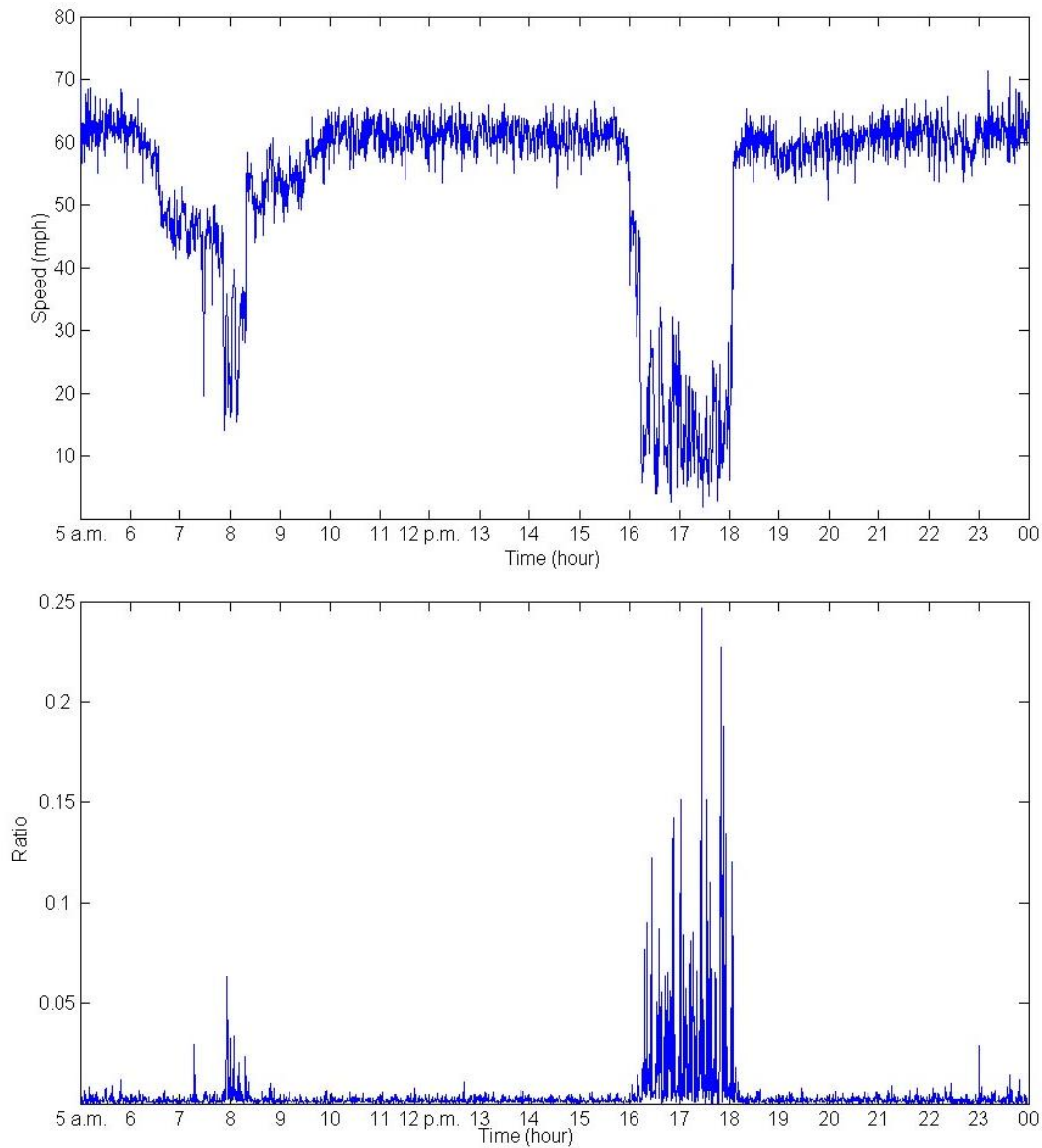


Figure 3.2 Speed and the ratio of speed variance to squared speed over time.

From this figure, it can be observed that the ratio σ_k^2 / \bar{s}_k^2 is almost negligible under normal traffic conditions. However, under congested traffic conditions with corresponding low speeds (\bar{s}_k), the ratio σ_k^2 / \bar{s}_k^2 becomes more significant. The maximum value of σ_k^2 / \bar{s}_k^2 is as high as 0.25. The example shows that speed variance sometimes are significant, and will have significant effects on speed estimation if ignored. High σ_k^2 / \bar{s}_k^2 values are generated when traffic congestion occurred.

3.2 THE UNSCENTED KALMAN FILTER (UKF)

As described in the literature review, although the EKF is able to deal with nonlinear problems, there are several issues regarding this method. A better approach to handle nonlinear systems is thus desirable for speed estimation. In this research project, a new method named the UKF is proposed for this problem.

Realizing the flaws existing in the EKF, Julier and Uhlmann (1996,1997, 2000) presented a new estimator—UKF. The UKF applies to nonlinear systems without the linearization steps required by the EKF. The UKF can achieve the second order or higher accuracy for nonlinear applications, and studies have shown the superiority of the UKF for nonlinear systems (van der Merwe et al., 2004; Shin and Naser, 2004; Wan and van der Merwe, 2000). The UKF have been applied to many problems such as state estimation, parameter estimation and machine learning, yet it was rarely used in the field of transportation.

Unscented transformation is the fundamental part of the UKF (Julier and Uhlmann, 1997). It uses a set of weighted points to parameterize the means and covariances of probability distributions. The set of points are called sigma points. They are selected according to a specific algorithm, not at random. To explain, consider propagating a random variable $x \in \mathfrak{R}^d$ through a nonlinear function $y = g(x)$. Assume the d -dimensional random variable x has mean \bar{x} and covariance P_x . To calculate the statistics of y , we form $2d + 1$ sigma points $\{\chi_0, \chi_1, \dots, \chi_{2d}\}$. The sigma points are calculated by

$$\begin{aligned} \chi_0 &= \bar{x} \\ \chi_i &= \bar{x} + \gamma(\sqrt{P_x})_i = \bar{x} + (\sqrt{(d+\kappa)P_x})_i & i=1, \dots, d \\ \chi_i &= \bar{x} - \gamma(\sqrt{P_x})_i = \bar{x} + (\sqrt{(d+\kappa)P_x})_i & i=d+1, \dots, 2d \end{aligned} \quad (3.1)$$

where

$\gamma = \sqrt{d + \kappa}$ = a scaling factor that determines the spread of sigma points around \bar{x} ;
 κ = provides an extra degree of freedom to fine-tune the higher order moments of the approximation; and
 $(\sqrt{(n + \kappa)P_x})_i$ = the i th column of the matrix square-root of $(n + \kappa)P_x$.

Once the sigma points are selected, they are propagated through the nonlinear function $Y_i = g(\chi_i), i = 0, 1, \dots, 2d$. Then the approximated mean, covariance and cross-variance of y are calculated by

$$\begin{aligned}
 \bar{y} &\approx \sum_{i=0}^{2d} w_i^{(m)} Y_i \\
 P_y &\approx \sum_{i=0}^{2d} \sum_{j=0}^{2d} w_{ij}^{(c)} Y_i Y_j^T \\
 P_{xy} &\approx \sum_{i=0}^{2d} \sum_{j=0}^{2d} w_{ij}^{(c)} \chi_i Y_j^T
 \end{aligned} \tag{3.2}$$

where $w_i^{(m)}$ and $w_{ij}^{(c)}$ are scalar weights of mean and covariance respectively. All weights should be equal or greater than zero. Figure 3.3 provides a schematic diagram of the unscented transformation.

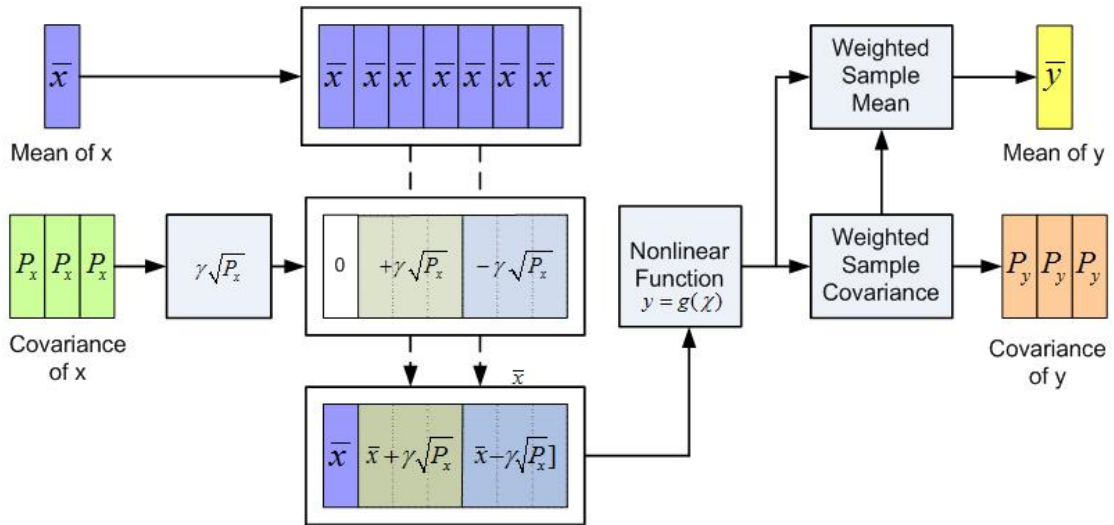


Figure 3.3 Unscented transformation of the UKF.

3.3 IMPLEMENTATION OF THE UKF ALGORITHM

In the implementation of the UKF, the state random variance is redefined as $x_k^\alpha = [x_k^T \ v_k^T \ n_k^T]^T$, where x_k is the original state, v_k is the process noise, n_k is the measurement noise. The sigma-point selection scheme in Equation 3.1 is applied to x_k^α to calculate the corresponding sigma points $\{\chi_{k,i}^\alpha; i=0,\dots,2d\}$, where $\chi_{k,i}^\alpha \in \mathfrak{R}^{d_x+d_v+d_n}$. The pseudo-code for the UKF is shown as follows (Julier and Uhlmann, 1997):

- Initialization.

$$\bar{x}_0 = E[x_0], \quad P_{x_0} = E[(x_0 - \bar{x}_0)(x_0 - \bar{x}_0)^T]$$

$$\bar{x}_0^\alpha = E[x_0^\alpha] = E[\bar{x}_0 \ 0 \ 0]^T$$

$$P_0^\alpha = E[(x_0^\alpha - \bar{x}_0^\alpha)(x_0^\alpha - \bar{x}_0^\alpha)^T] = \begin{pmatrix} P_{x_0} & 0 & 0 \\ 0 & R_v & 0 \\ 0 & 0 & R_n \end{pmatrix}$$

where $x_0^\alpha = [x_0 \ v_0 \ n_0]^T$, v denotes the process noise variable, and u is the measurement noise variable; correspondingly, R_v is the covariance of v , and R_n is the covariance of n .

- For time intervals $k = 1, \dots, \infty$

- 1) Calculation of sigma points.

$$\chi_{k-1}^\alpha = [\bar{x}_{k-1}^\alpha \ \bar{x}_{k-1}^\alpha + \gamma\sqrt{P_{k-1}^\alpha} \ \bar{x}_{k-1}^\alpha - \gamma\sqrt{P_{k-1}^\alpha}]$$

- 2) Time update.

$$\chi_{k|k-1}^x = f(\chi_{k-1}^x, \chi_{k-1}^v)$$

$$\bar{x}_k^- = \sum_{i=0}^{2d} w_i^{(m)} \chi_{i,k|k-1}^x$$

$$P_{x_k}^- = \sum_{i=0}^{2d} w_i^{(c)} (\chi_{i,k|k-1}^x - \bar{x}_k^-)(\chi_{i,k|k-1}^x - \bar{x}_k^-)^T$$

where $\chi_k^\alpha = [(\chi^x)^T \ (\chi^v)^T \ (\chi^n)^T]^T$, $w_i^{(m)}$ is again the weight of mean and $w_i^{(c)}$ denotes the weight of covariance for the i th sigma point.

- 3) Measurement update.

$$\begin{aligned}
\mathbf{y}_{k|k-1} &= \mathbf{h}(\mathcal{X}_{k|k-1}^x, \mathcal{X}_{k-1}^u) \\
\bar{y}_k^- &= \sum_{i=0}^{2d} w_i^{(m)} y_{i,k|k-1} \\
P_{\bar{y}_k} &= \sum_{i=0}^{2d} w_i^{(e)} (\mathbf{y}_{i,k|k-1} - \bar{y}_k^-)(\mathbf{y}_{i,k|k-1} - \bar{y}_k^-)^T \\
P_{x_k y_k} &= \sum_{i=0}^{2d} w_i^{(e)} (\mathcal{X}_{i,k|k-1}^x - \bar{x}_k^-)(\mathbf{y}_{i,k|k-1} - \bar{y}_k^-)^T \\
K_k &= P_{x_k y_k} P_{\bar{y}_k}^{-1} \\
\bar{x}_k &= \bar{x}_k^- + K_k (y_k - \bar{y}_k^-) \\
P_{x_k} &= P_{x_k}^- - K_k P_{\bar{y}_k} K_k^T
\end{aligned}$$

where y_k is the measurement, $h(\cdot)$ is the function described in Equation 2.2 denoting the relationship between observations and states, and K_k is the Kalman gain.

In the application of speed estimation, speed (\bar{s}_k) denotes x_k , the ratio of occupancy over traffic count (O_k / N_k) denotes the measurement y_k , the speed variance (σ_k^2) is the state noise covariance R_v , and the variance of $\{O_i / N_i; i = 1, \dots, k\}$ is set as the observation noise covariance (R_n) exponentially. As the speed variance σ_k^2 cannot be obtained using detector outputs, a common value is used in applications, which is determined by experiments.

CHAPTER 4. RESULTS AND DISCUSSION

This chapter provides results of speed estimation using the UKF method. The data sources for applications are first described. Data from ADR-6000 detectors and dual-loop detectors are adopted for speed estimation, result analysis, and evaluation.

4.1 DATA SOURCES

As described in chapter 2, single loop detectors, double loop detectors, and Peek ADR-6000 detectors can generate outputs for the study of speed estimation. Since single loop detectors do not have the output of speed, it is not feasible to evaluate estimation results if no other sources of data are available at the site for the same duration. Thus, data from both double loop and ADR-6000 detectors are collected for the purpose of this project.

4.1.1 ADR-6000 Data

With a purpose of evaluating vehicle detectors, Texas Transportation Institute (TTI) has installed various representative detectors at two freeway test beds. One is located on State Highway 6 (S.H.6) in College Station, Texas; the other is on Interstate Highway 35 (IH-35) near the 47th street in Austin, Texas. S.H.6 has four lanes with 2 each in the northbound and southbound directions. IH-35 has four lanes in the southbound direction. These two locations use Peek ADR-6000 inductive loops for baseline data in each lane. ADR-6000 detectors output data for each vehicle passing over. The data include vehicle speed, length, presence time, and classification. A sample of output data is shown in Table 4.1, in which the time duration is 2 minutes. It is easy to calculate occupancy and traffic count for each time interval based on ADR-6000 outputs through using records of detection time and presence time.

In addition to high accuracy of detection of ADR-6000 detectors, there is another advantage of using such data. Single loop detectors output data every time interval. The most commonly used durations of time intervals are 20 seconds, 30 seconds, and 1 minute. Using the outputs of ADR-6000 data, it is easy to compile data into different output intervals as needed. Therefore, ADR-6000 detector data from a location enable one to do speed estimation using different types of time intervals. This task cannot be done using double loop detectors since they produce aggregate output with a pooled interval.

Table 4.1 Sample Data of ADR-6000 Outputs

Date	Detection Time	Vehicle Length (m)	Speed (m/s)	Presence Time (sec.)	Vehicle Classification
27/01/04	9:00:01	5.39	33.22	0.259	3
27/01/04	9:00:08	4.47	38.35	0.178	2
27/01/04	9:00:11	4.56	37.6	0.207	2
27/01/04	9:00:28	4.56	31.79	0.228	2
27/01/04	9:00:35	5.16	32.6	0.239	2
27/01/04	9:00:45	4.17	34.17	0.218	2
27/01/04	9:00:46	4.93	34.28	0.228	2
27/01/04	9:00:52	5.13	34.49	0.209	2
27/01/04	9:01:01	5.52	33.95	0.239	3
27/01/04	9:01:06	12.75	33.09	0.496	8
27/01/04	9:01:08	18.64	33.04	0.651	9
27/01/04	9:01:12	5.6	32.82	0.261	3
27/01/04	9:01:13	5.95	33.52	0.27	5
27/01/04	9:01:14	6.15	33.5	0.259	5
27/01/04	9:01:16	4.27	34.73	0.209	2
27/01/04	9:01:19	4.33	31.72	0.238	2
27/01/04	9:01:25	4.8	35.3	0.228	2
27/01/04	9:01:26	5.49	33.88	0.26	3
27/01/04	9:01:49	4.56	38.62	0.197	2
27/01/04	9:01:55	4.34	35.62	0.208	2

4.1.2 Dual-Loop Data

The city of San Antonio in Texas has a good freeway system, with three interstate highways (IH-35, IH-37, and I-10) passing through the city. Many dual loops are installed on these highways within the city limits and provide data for efficient transportation management

systems. Dual loop data were downloaded from the San Antonio Texas Transportation Institute server for this research project. The location of dual loops is on IH-35 at Seguin Road, with 3 lanes in the northbound direction. The length of time intervals is 20 seconds. Speed, occupancy, and count data were collected at this location.

4.2 APPLICATIONS

With data collected from those three locations, the UKF as well as some other existing methods are applied to estimate speed and to compare results. In this section, datasets from these three locations are used. The datasets are described as follows:

- 1) Peek ADR-6000 detector data on S.H.6 in College Station. A weekday dataset was collected on January 27, 2004 from the northbound S.H.6 test bed. It is found that the shoulder lane (numbered as lane 1) has a daily traffic volume of 12975 vehicles and 7% trucks with 3-axle or more during the entire day; the median lane (numbered as lane 2) has around 10000 vehicles and 4.5% trucks. Figure 4.1 shows hourly traffic volumes of this dataset. As the truck percentage and the daily traffic volume are relatively low in the median lane, only lane 1 is used for speed estimation. Note that lanes are numbered from the outmost lane to the innermost lane in this project.

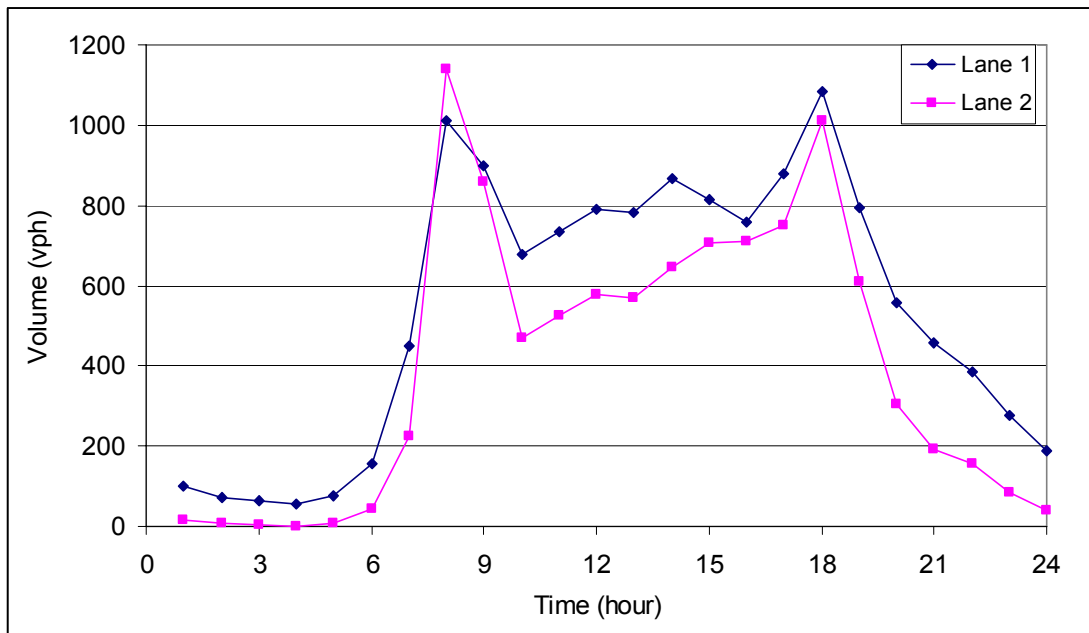


Figure 4.1 Hourly traffic volumes on SH6 in College Station (Jan. 27, 2004).

- 2) Peek ADR-6000 detector data on IH-35 in Austin. Two weekday datasets were collected on October 27 and November 9, 2004 from the 4 southbound lanes. Daily traffic volumes from lane 1 through lane 4 on Oct. 27 are 27670, 24936, 20226, and 13850 vehicles. Correspondingly the truck percentages are 12.3%, 5.3%, 1.9%, and 2.8%. A plot of hourly traffic volumes on Oct. 27 is shown in Figure 4.2. The traffic flow pattern in lane 1 is much similar to lane 2. These two datasets are used for speed estimation.

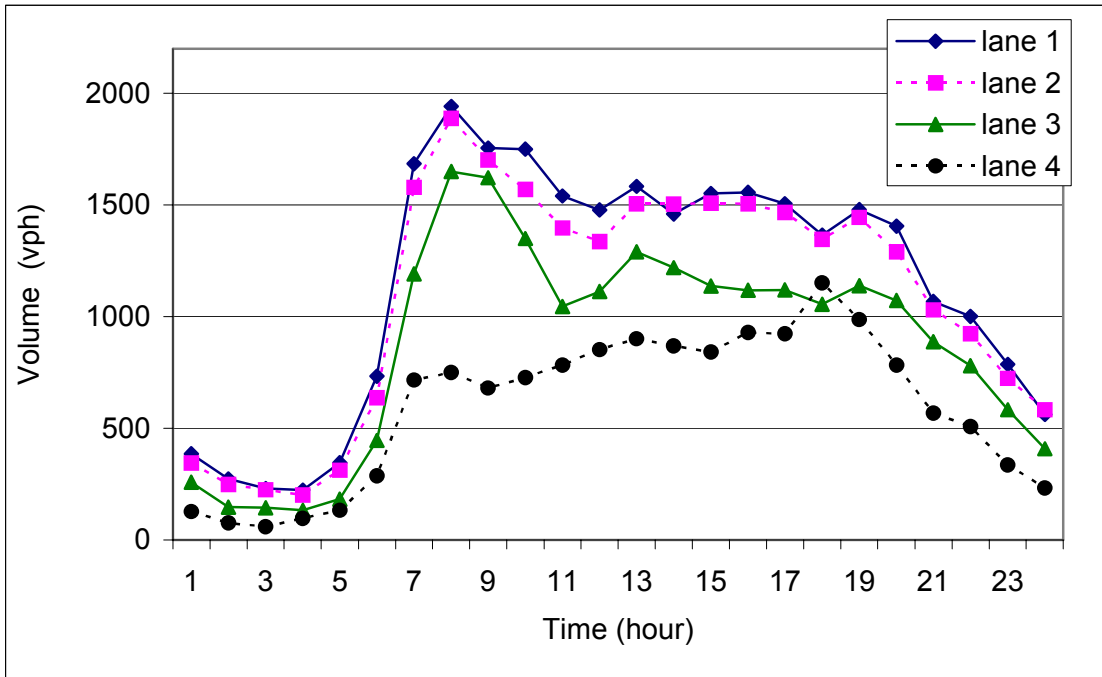


Figure 4.2 Hourly traffic volumes on IH-35 in Austin (Oct. 27, 2004).

- 3) Double loop detector data on IH-35 in San Antonio. One week's data from February 10-16, 2003 (Monday through Sunday) are collected from lane 1 (the outmost lane) of the northbound direction. After data collection, records with zero count or occupancy are removed from the original dataset. Daily traffic volumes in those seven days are 18937, 18034, 16727, 17244, 22089, 15889, and 12484 vehicles from Monday to Sunday. Figure 4.3 shows hourly traffic volumes over this week.

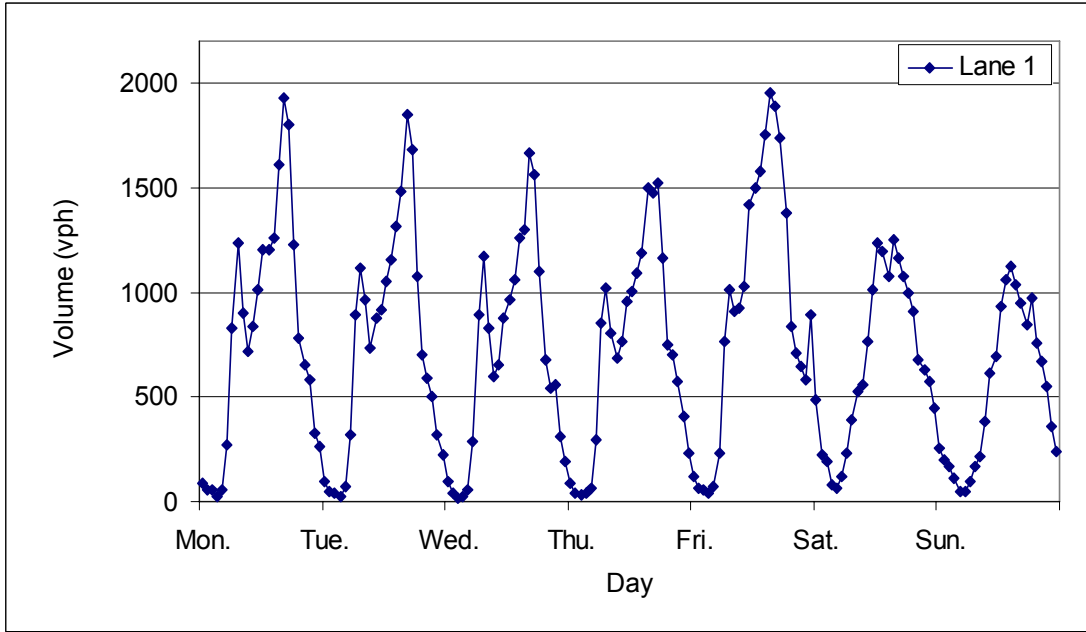


Figure 4.3 Hourly traffic volumes on IH-35 in San Antonio (Feb. 10-16, 2004).

The UKF algorithm is first implemented to those four datasets. Estimated results and measured speed data from detectors are plotted in Figures 4.4 through 4.13. In Figures 4.4 through 4.12, the duration of each time interval is 30 seconds; in Figure 4.9, the duration is 20 seconds. Figure 4.4 represents the first dataset, Figures 4.5 through 4.8 refer to the second dataset, Figures 4.9 through 4.12 are for the third dataset, and Figure 4.13 refers to the fourth dataset. Since the intervals that have zero traffic counts are removed, the total number of time intervals during one day may be different from lane to lane and location to location. Mean Absolute Errors (MAEs) and Root Mean Square Errors (RMSEs) are generated to evaluate speed estimation accuracy. The RMSE is the square root of Mean Square Error (MSE), which can capture both the variance of errors and the bias of estimates. The MAE and RMSE are derived as described in the following equations:

$$MAE = \frac{1}{M} \sum_{k=1}^M |\hat{s}_k - s_k| \quad (4.1)$$

$$RMSE = \sqrt{\frac{1}{M} \sum_{k=1}^M [\hat{s}_k - s_k]^2} \quad (4.2)$$

where M is the total number of time intervals, \hat{s}_k is the estimated speed of the k th time interval, and s_k is the observed speed of the k th time interval. The MAEs and RMSEs are also shown in the figures.

For the first dataset, traffic speeds were at around 65 mph throughout the day (Figure 4.4). From Figure 4.1, it can be seen that the peak hour (7:00-8:00 and 17:00-18:00) traffic volumes were only around 1000 vehicles per hour. No congestion existed during the entire day. The UKF has good results of speed estimation, as indicated by the MAE (3.62 mph) and the RMSE (4.53 mph). The estimated speeds have relatively large variations during the first few hours. This may be explained by the fact that truck percentages are high during this time period.

The speed estimation results for the second dataset are shown in Figures 4.5 through 4.8. The estimated results become increasingly better from lane 1 to lane 4. This phenomenon is mainly due to the differences of truck percentages and traffic volumes among those lanes. Traffic congestions existed during the morning and afternoon peak hours, and traffic speeds were low in lanes 1 through 3 during traffic congestion. Even under the low observed speed condition, the estimated speeds can still capture real speed patterns very well. During the first few hours, the estimated speeds have large fluctuations even though traffic is under free flow conditions. This again is due to the high percentages of trucks during this time period. As a result, the true speeds tend to be underestimated.

The third dataset came from the same place as the second dataset, but was collected during a different time. From the observed speed curves shown in Figures 4.9 through 4.12, it can be seen that traffic congestion during after peak hours lasts a longer time period than that of the second dataset. Speeds in some cases are less than 10 mph. Observed speed curves during morning peak hours exhibit similar patterns as those of the second dataset. The UKF again has good performances.

The fourth dataset enables us to observe the performance of the UKF throughout multiple days. Estimated results shown in Figure 4.13 again demonstrate the accurate estimations of the UKF. The estimated speeds follow the measured speeds very well. An observation into dual-loop data finds that measured speeds sometimes are very high during nighttime. The highest measured average speed during a time interval is 150 mph with two vehicles detected. Such high speed data might have not been accurately measured based on other measurements (traffic count and occupancy). However, such erroneous data do not evidently affect speed estimation.

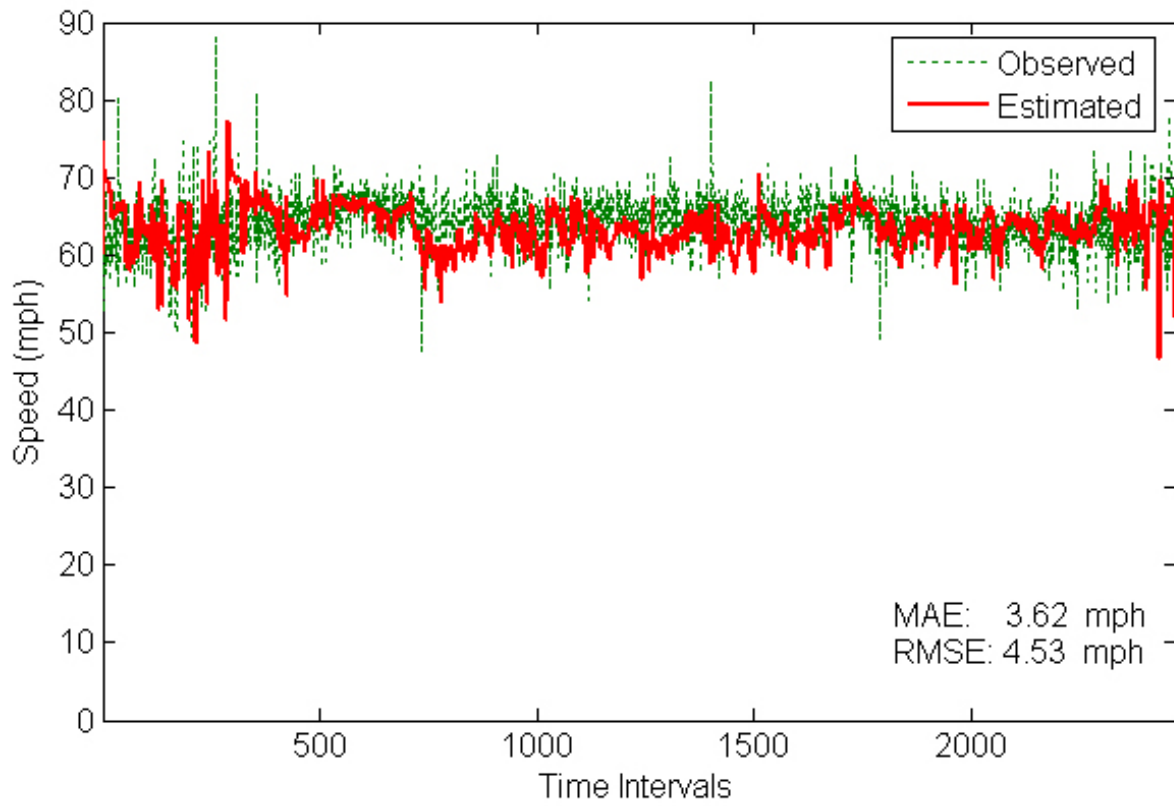


Figure 4.4 Estimated speeds by the UKF on S.H.6 (Jan. 27, 2004).

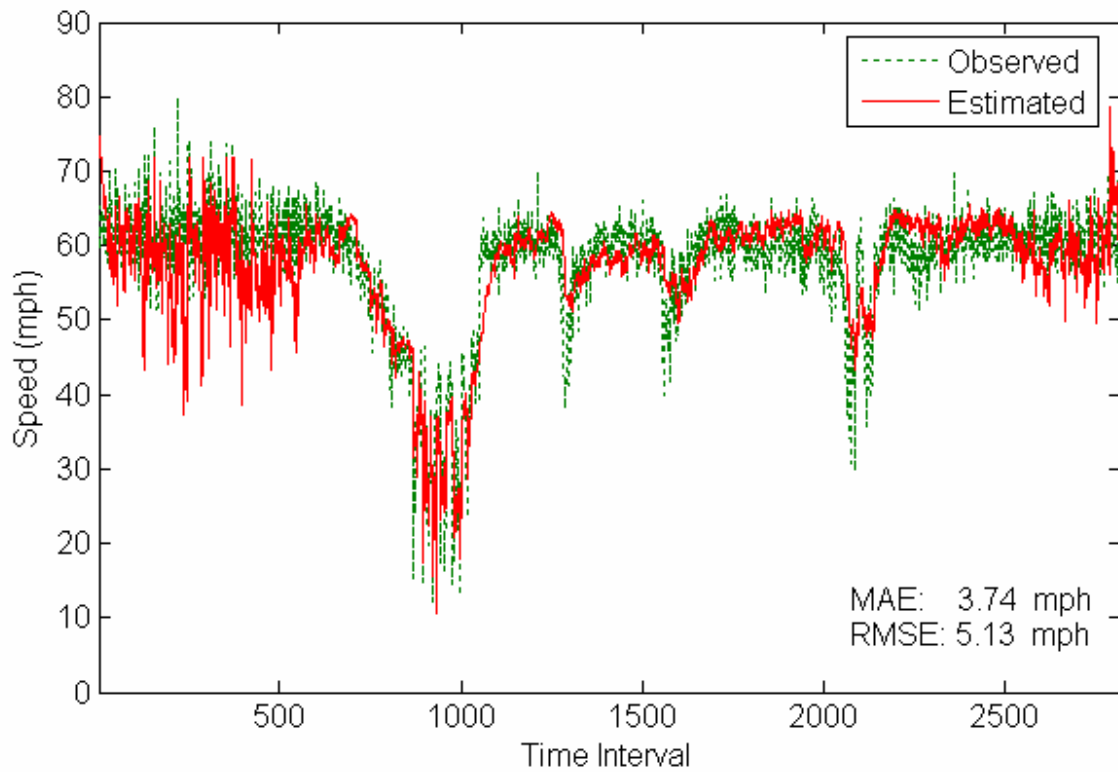


Figure 4.5 Estimated speeds by the UKF on IH-35 in Austin (Lane 1, Oct. 27, 2004).

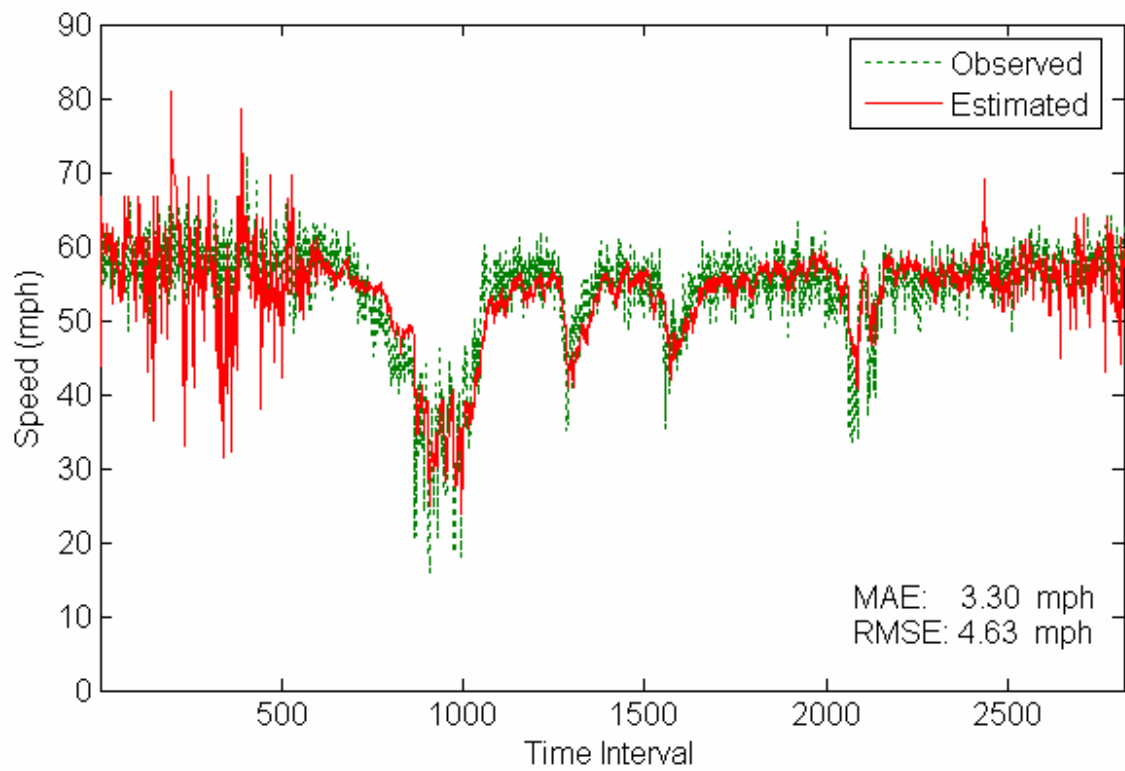


Figure 4.6 Estimated speeds by the UKF on IH-35 in Austin (Lane 2, Oct. 27, 2004).

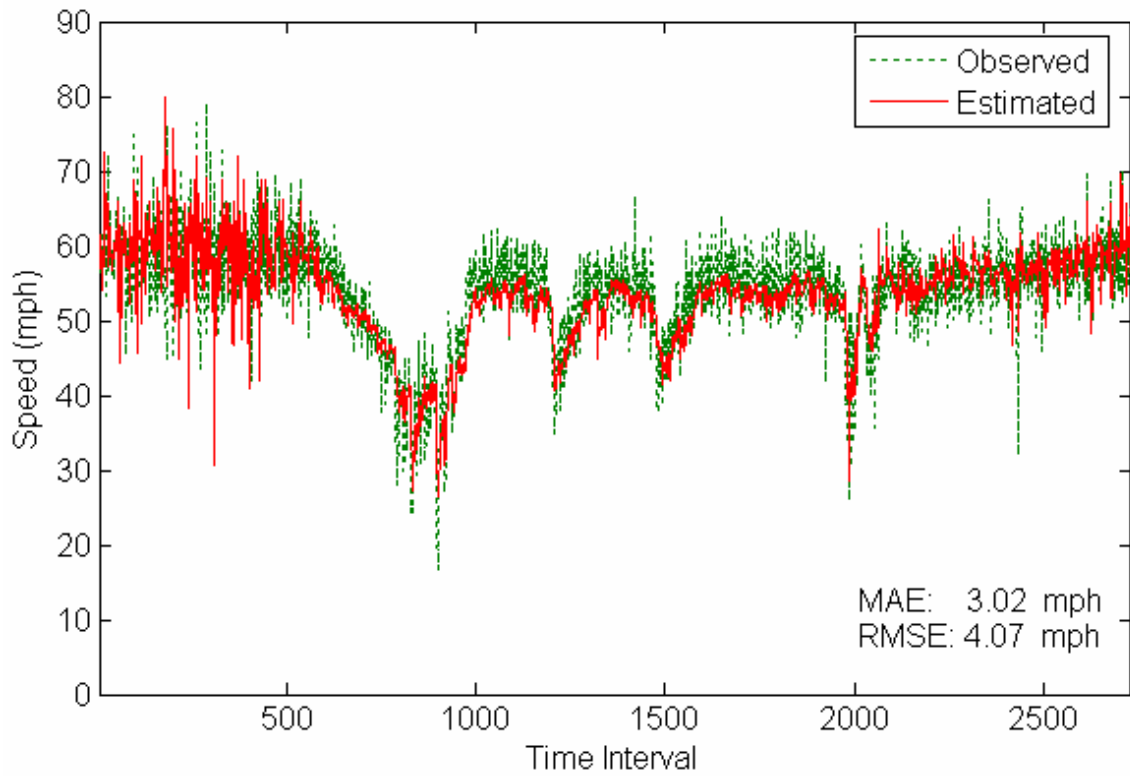


Figure 4.7 Estimated speeds by the UKF on IH-35 in Austin (Lane 3, Oct. 27, 2004).

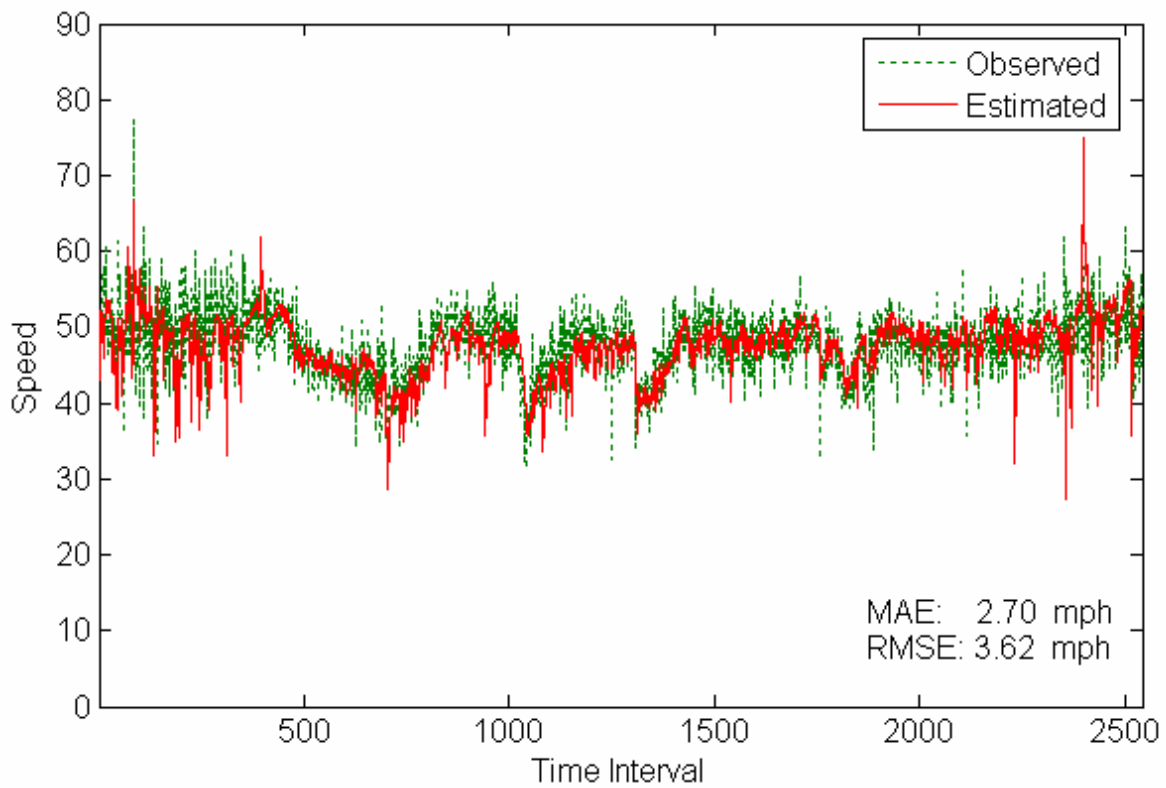


Figure 4.8 Estimated speeds by the UKF on IH-35 in Austin (Lane 4, Oct. 27, 2004).

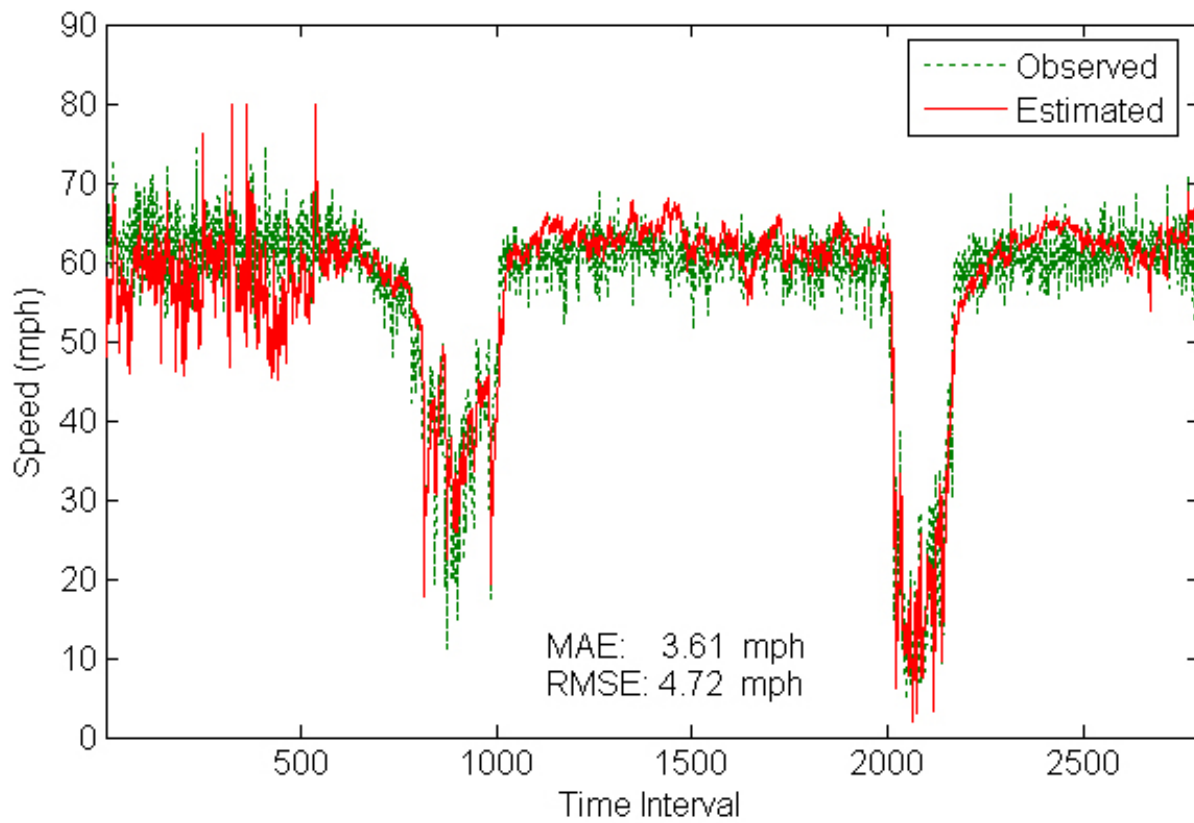


Figure 4.9 Estimated speeds by the UKF on IH-35 in Austin (Lane 1, Nov. 09, 2004).

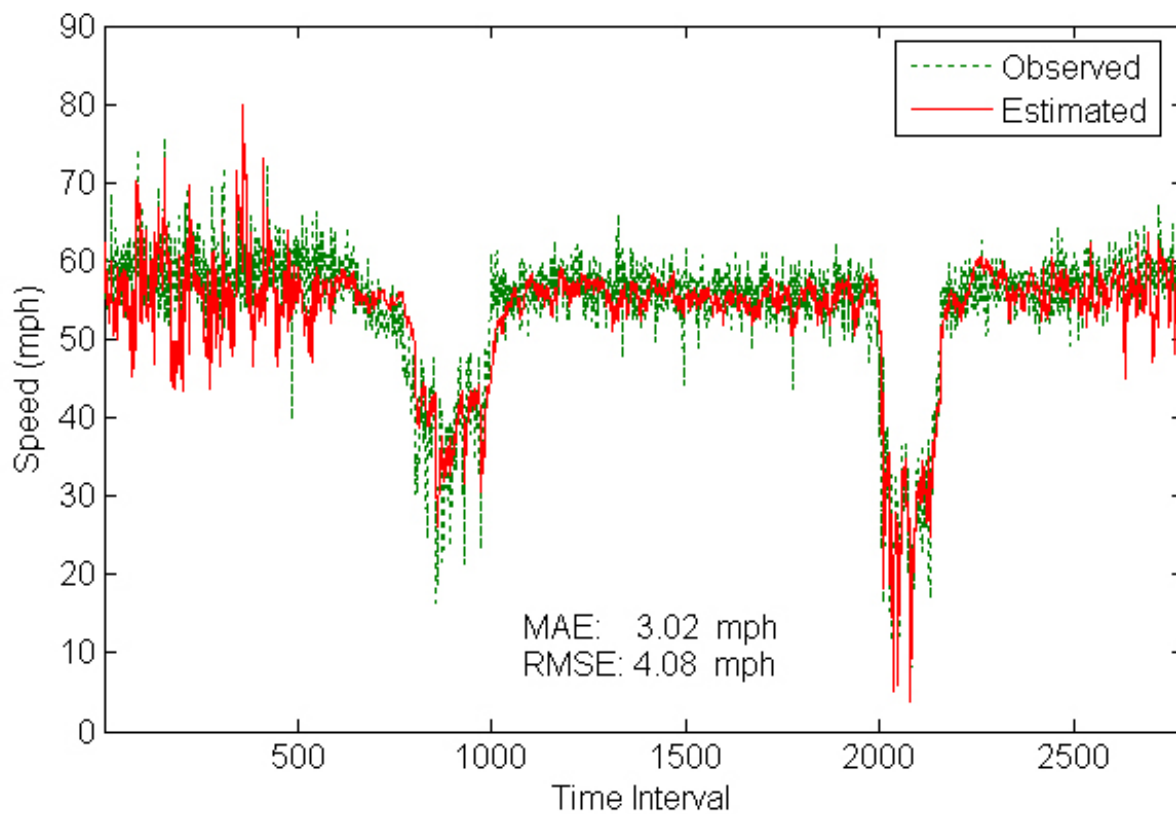


Figure 4.10 Estimated speeds by the UKF on IH-35 in Austin (Lane 2, Nov. 09, 2004).

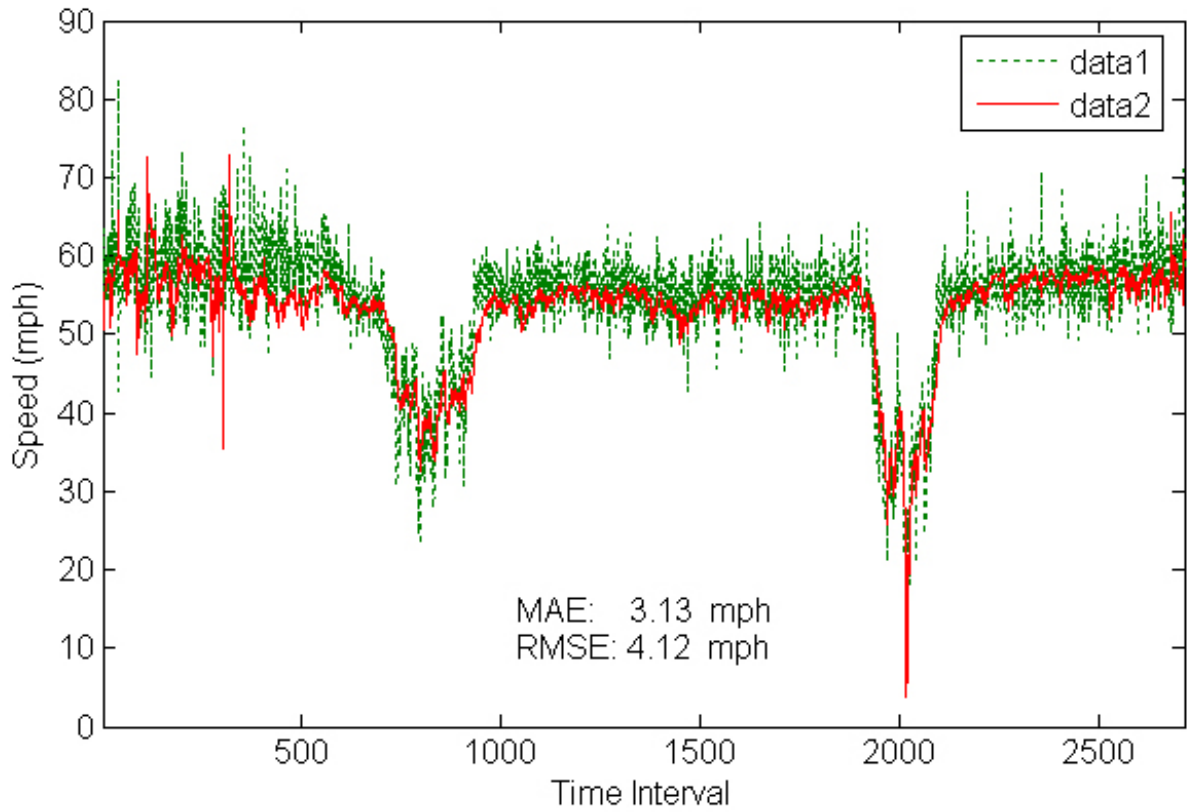


Figure 4.11 Estimated speeds by the UKF on IH-35 in Austin (Lane 3, Nov. 09, 2004).

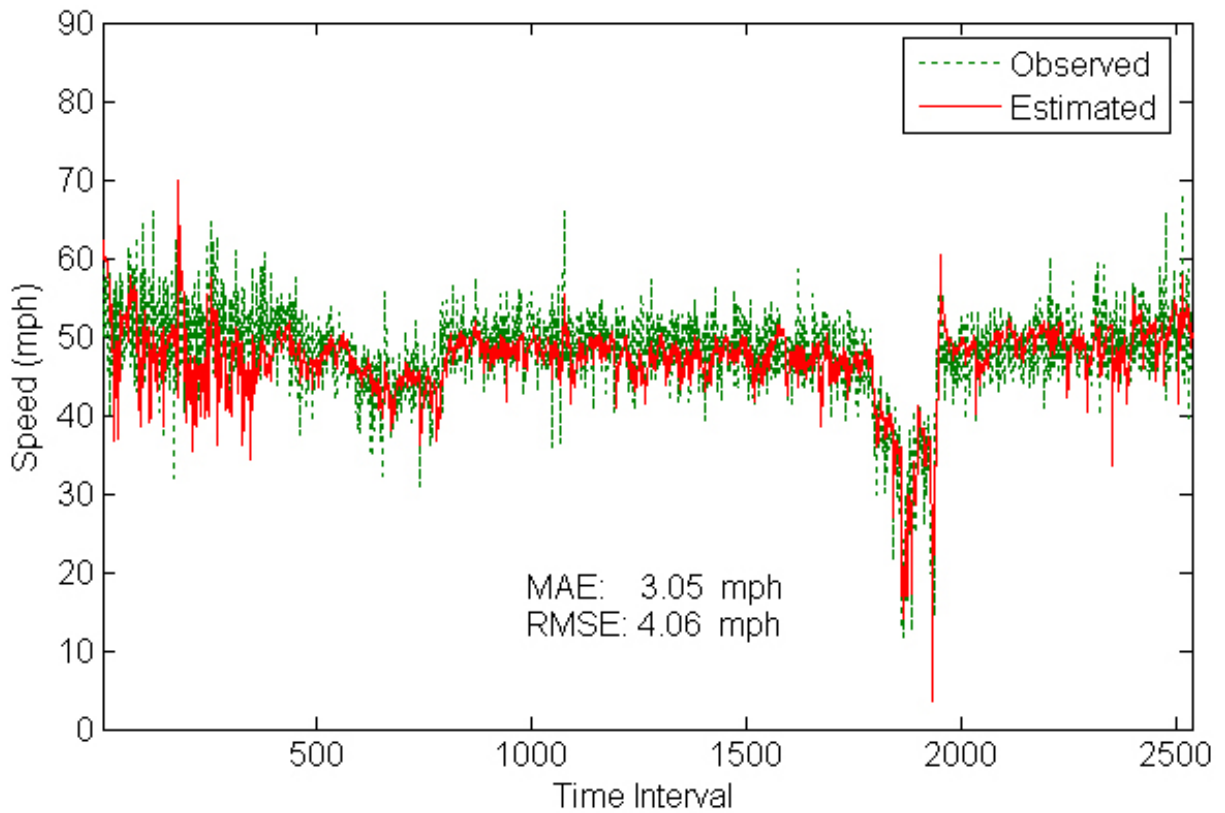


Figure 4.12 Estimated speeds by the UKF on IH-35 in Austin (Lane 2, Nov. 09, 2004).

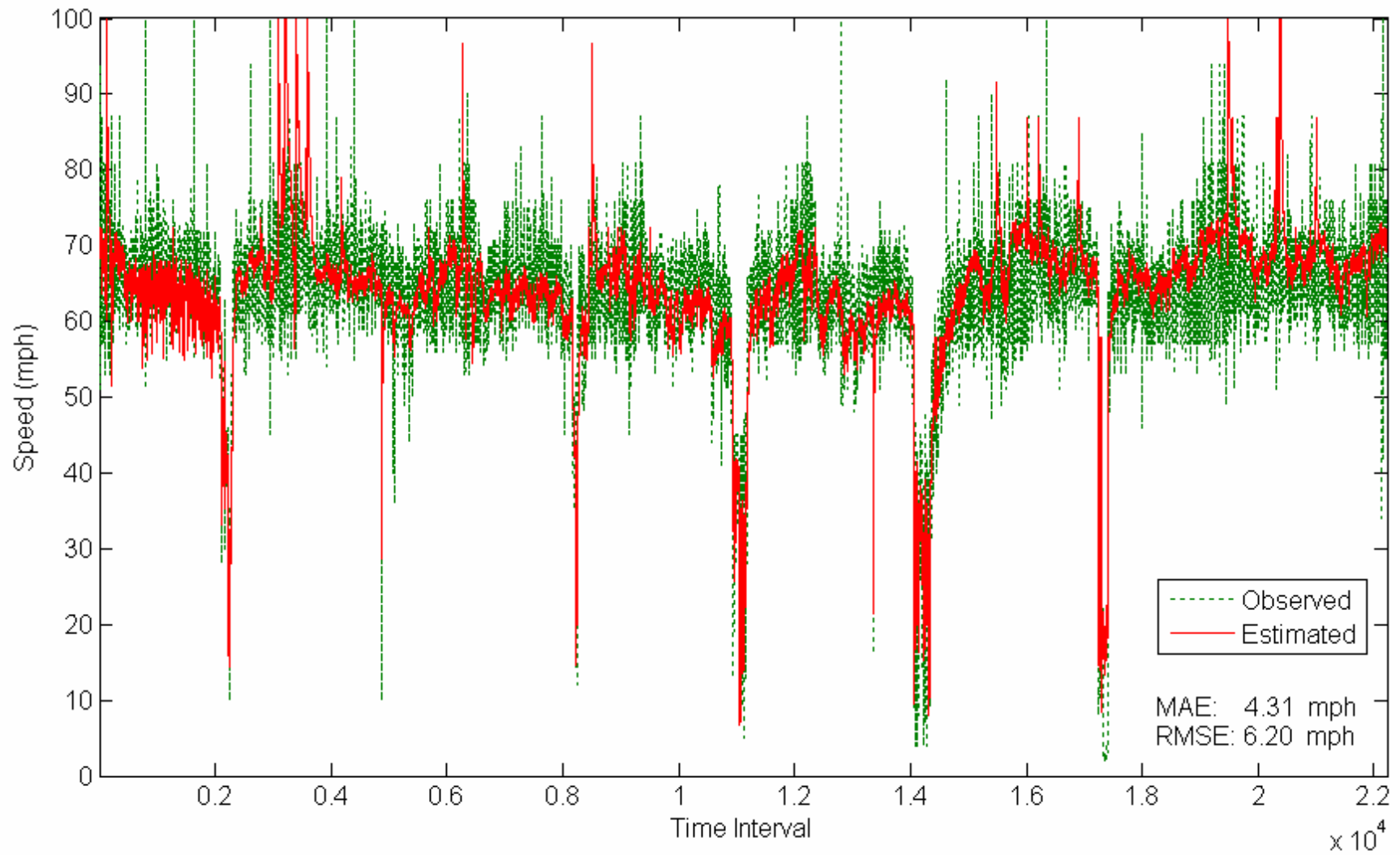


Figure 4.13 Estimated speeds by UKF on IH-35 in San Antonio (Lane 1, Feb.10-16, 2003).

To examine the performance of the UKF under congested traffic conditions, a portion of Figure 4.9 from the 1900th time interval to the 2200th time interval that includes the afternoon peak hours is enlarged and shown in Figure 4.14. It can be observed that the UKF captures speed variations well even under congested conditions. The UKF does not display evidently delayed responses to real speeds. Delayed responses in many cases are the limitations of Kalman Filters.

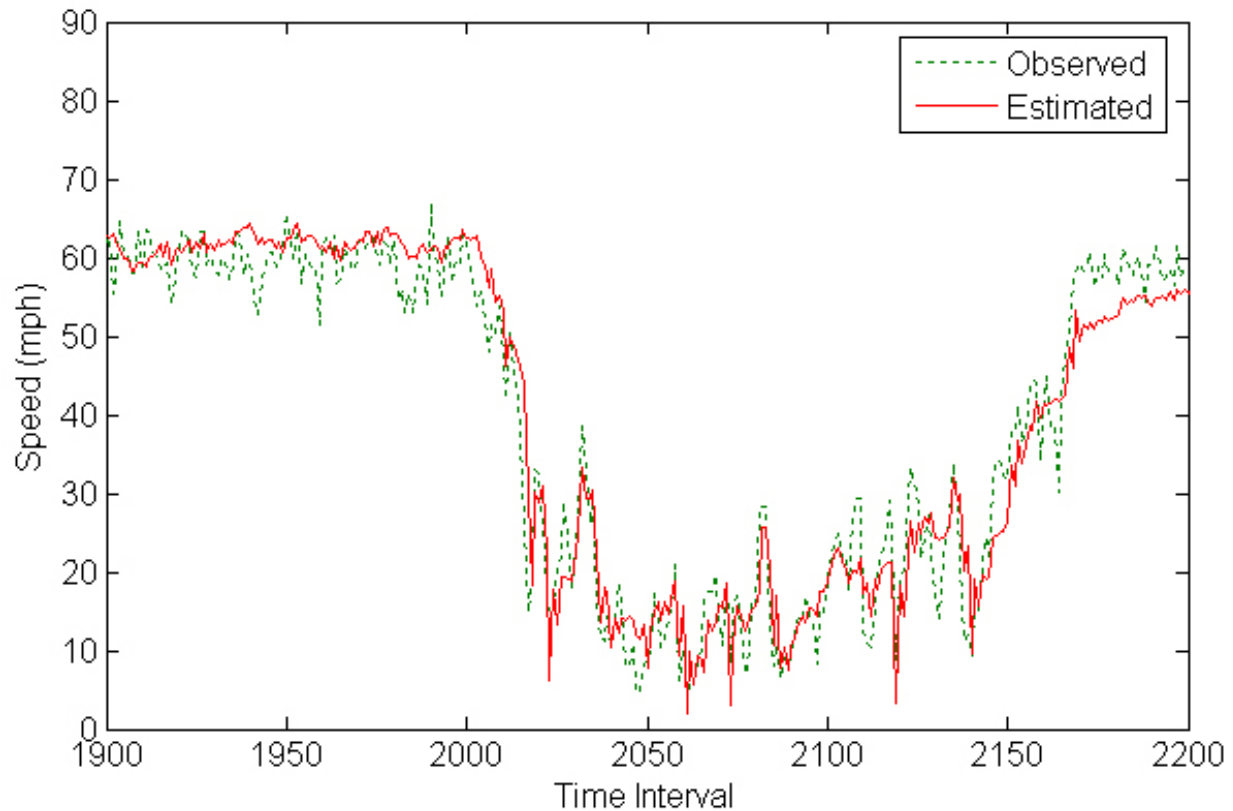


Figure 4.14 Speed estimation under congested traffic conditions on IH-35 in Austin (Nov. 09, 2004).

To further evaluate the accuracy of speed estimation by the UKF, the EKF method is also applied to those datasets. Estimation results from both methods are shown in Table 4.2. MAEs and RMSEs are used for the comparison.

Table 4.2 Comparison of Speed Estimation Results

Location	Date	Lane No.	EKF		UKF	
			MAE (mph)	RMSE (mph)	MAE (mph)	RMSE (mph)
S.H.6 in College Station						
	Jan.27,2004	Lane 1	4.85	6.23	3.62	4.53
IH-35 in Austin						
	Oct.27, 2004	Lane 1	7.36	10.17	3.74	5.13
		Lane 2	7.03	10.05	3.30	4.63
		Lane 3	5.18	7.00	3.02	4.07
		Lane 4	4.18	5.6	2.70	3.62
	Nov.09, 2004	Lane 1	5.65	7.24	3.61	4.72
		Lane 2	5.27	7.16	3.12	4.08
		Lane 3	4.59	5.91	3.13	4.1
		Lane 4	4.91	6.74	3.05	4.06
IH-35 in San Antonio						
	Feb.10-16, 2003	Lane 1	6.90	8.63	4.31	6.20

From the table, it can be seen that the UKF method has consistently better estimates than the EKF. Taking the second dataset (IH-35 in Austin on Oct. 27, 2004) as an example, the EKF has much larger MAEs and RMSEs than the UKF, which means that the EKF has larger biases and error variances. The UKF thus generates more accurate and stable estimates. From lane 1 to lane 4, the estimation results from the EKF have a similar tendency as those from the UKF: estimation accuracies become better from lane 1 to lane 4. Figure 4.15 presents an example of speed estimation using the EKF method for lane 3 of the second dataset. A closer observation shows that the EKF has delayed responses to speed variations.

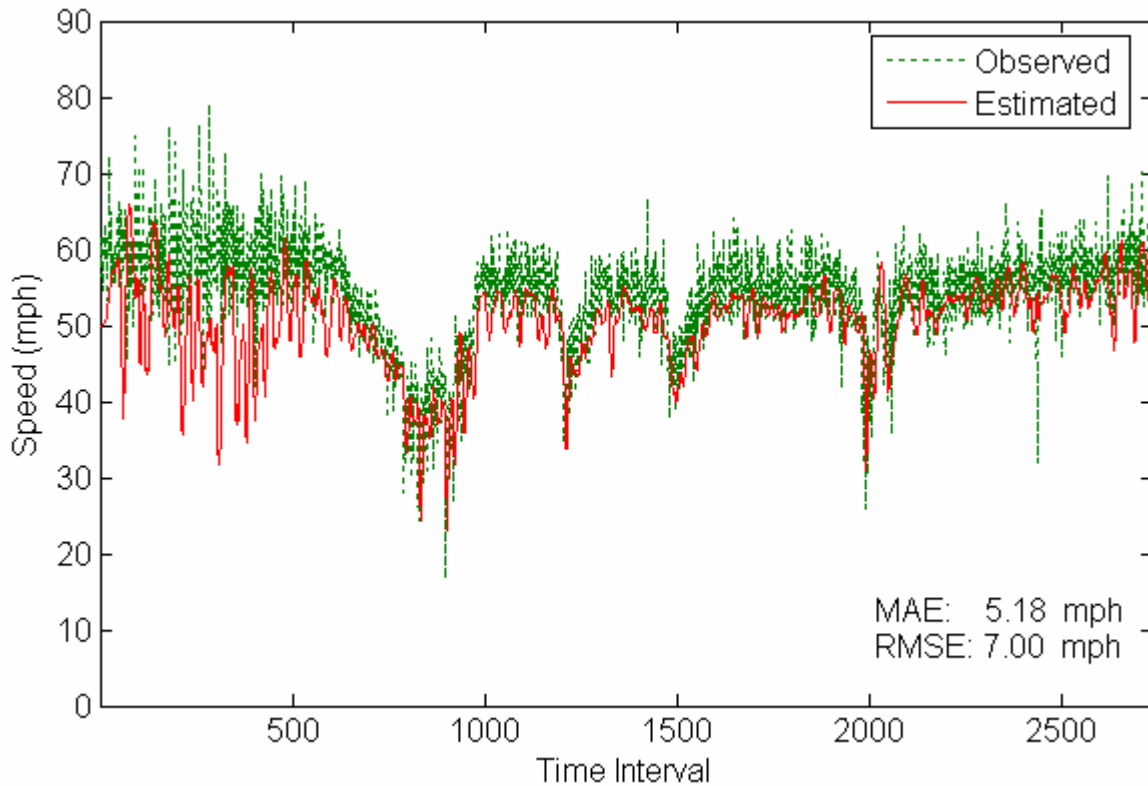


Figure 4.15 Estimated speeds by the EKF on IH-35 in Austin (Lane 3, Oct. 27, 2004).

It should be noted that the speed estimated by both the UKF and the EKF is time mean speed, while the speed estimated by the g-estimator method is space mean speed (Rakha and Zhang, 2005). In practice, speeds measured from double loops and ADR-6000 detectors are time mean speeds. Therefore, the accuracies of speed estimation using the EKF and the UKF can be validated by comparing estimated speeds with measured speeds. May (1990) and Rakha and Zhang (2005) explored the difference between space mean speed and time mean speed estimates. The authors concluded that they are rather close under normal conditions, while large differences were observed during congestion. Based on the conclusion, we are able to compare estimation results from the g-estimator with those from the UKF and/or the EKF under normal traffic conditions. As can be seen from Figure 4.4, the first dataset displays normal traffic conditions and can be used for such comparison. The g-estimator method is also applied to this dataset. The MAE and RMSE of this method are 8.97 mph and 12.35 mph, respectively. As expected, the g-estimator method has much worse performance than the EKF and the UKF.

4.3 REQUIREMENTS FOR IMPLEMENTATIONS

In order to implement an algorithm in speed estimation, certain requirements, such as initialization and parameter settings, are required. The requirements vary from method to method and represent the degree of difficulties in real-time applications. This section is thus to identify and discuss the requirements for the implementations of speed estimation methods, which include the g-estimator, the EKF and the UKF.

The g-estimator method is the simplest approach. It only requires a common g value, which is the reciprocal of the MEVL. However, this method has been shown to have poor performances for speed estimation.

The EKF and the UKF have similar requirements, including the constant MEVL, the process noise (v), the measurement noise (n) and the parameters (a and b in Equation 2.9) for state-transition. In the EKF, the noises and the parameters are experientially set as constant values. As has been mentioned, the parameters a and b are derived using Auto Regression (AR) method with 2 orders based on measured speed data.

In the UKF, the process noise represents the standard deviation of speed variance, denoted by σ_s . As speed variance cannot be derived from single loop outputs, it is set as a constant during estimation. To examine the sensitivity of speed variance on estimation results, additional experiments are conducted using lane 1 data of the second dataset. Different values of σ_s , ranging from 0.1 to 8, are assigned. Results of MAEs and RMSEs are shown in Figure 4.16. It is found that speed variance does not affect results significantly.

In addition to speed variance (state noise), the measurement noise ($\sigma_{O/N}^2$) is also considered in the implementation. As in the EKF, measurement noises in the UKF are determined experientially. In the UKF, the current measurement noise (σ_{O_k/N_k}^2) can be determined recursively by the variance of measurements based on last noise value ($\sigma_{O_{k-1}/N_{k-1}}^2$) and the current measurement (O_k / N_k). Thus, it is an easy and efficient way to account for the measurement noise.

Finally, the parameters (a and b) in the UKF are simply set as the same values, that is $a = b = 0.5$. The determination of a and b in the UKF is thus easier than in the EKF.

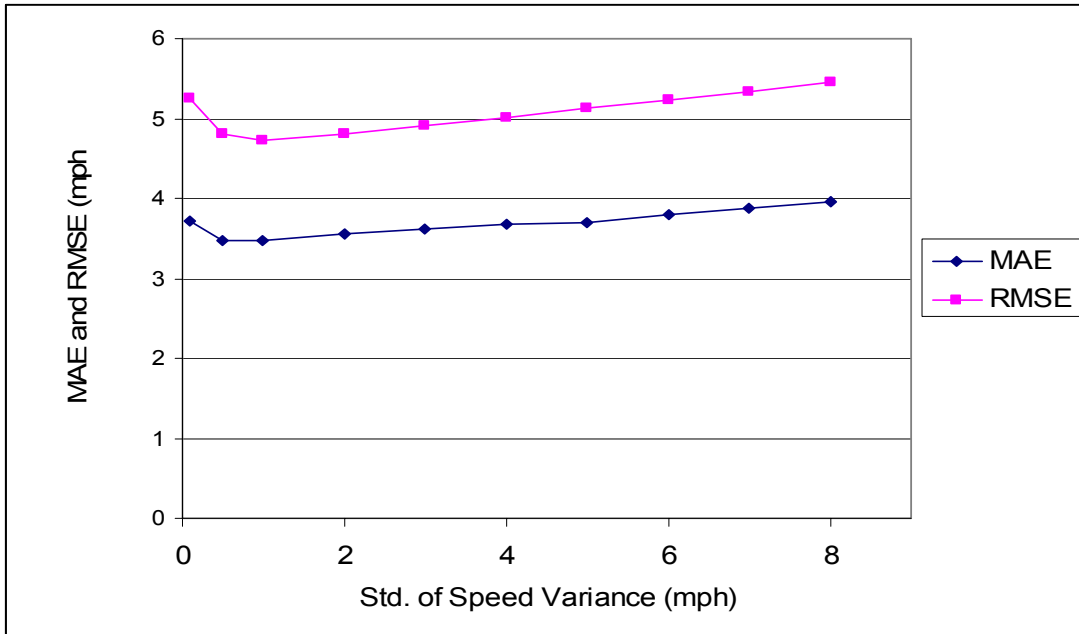


Figure 4.16 Sensitivity analysis of speed variance on estimation results on IH-35 in Austin (Lane 1, Oct. 27, 2004).

CHAPTER 5. ESTIAMIION OF LARGE TRUCK VOLUME

Based on previous experiments, speed can be accurately estimated using single loop outputs through the implementation of the UKF algorithm. With accurate speeds available, the information of the average vehicle length at each time interval can be derived. And this motivates the development of a method to estimate large truck volume. Here, a Large Truck (LT) or a long vehicle is defined as a truck with a length greater than or equal to 12.19 m (40 feet) as suggested in the studies of Wang and Nihan (2001) and Kwon et al. (2002).

5.1 INTRODUCTION

Truck traffic has been steadily increasing on America's highways due to the growing economy and increased international trade. The Vehicle Inventory and Use Survey (VIUS), conducted every 5 years by the U.S. Census Bureau, reported that over 89 million trucks were registered in the U.S. in 2002, with a nearly 19% increase from 75 million trucks in 1997 (U.S. Census Bureau, 1998 and 2004). Trucks have different characteristics from passenger cars and thus are a key consideration in many stages of a highway project. Trucks are critical to transportation planning, pavement design, geometric design, and traffic operations. For instance, many geometric criteria in the Green Book (AASHTO, 2001) take truck characteristics into account. With the rapid growth of truck volumes on highways, safety with respect to trucks has also received more and more attention.

Research in the estimation of large truck volume from single loop outputs has attracted more and more attention in recent years. A study in the state of Washington (Wang and Nihan, 2001) proposed a pattern discrimination method to estimate large truck volume using single loop data. One assumption used in that study is that vehicle speeds in each five-minute time period are consistent and speed variance can be ignored. The developed method is hence suitable for stable traffic conditions without large speed variations. Another study in California (Kwon et al., 2002) used lane-to-lane speed correlation to estimate large truck volume using data from single loop detectors. They assumed that the percentage of large trucks in the leftmost lane can be ignored, and vehicle speeds over different lanes tend to be synchronized. However, due to wide ranges of traffic and geometric conditions, variations of speeds and truck lane distribution can be very significant. The assumptions made in the prior studies may not be valid for some types or locations of highways or for some traffic conditions. This drawback limits the application scope

and may affect the effectiveness of the approach. Most recently, an Artificial Neural Network (ANN) was proposed for vehicle classification using single loop outputs (Zhang et al., 2005). Four length-based vehicle classification categories were used in this study. The results showed that this method performs well for two categories with the shortest and the largest vehicle lengths. The performance of an ANN is directly related to the training dataset that is used, and overprediction based on limited training data is often associated with ANNs.

In this study, an algorithm is developed based on the information of the MEVL, which can be derived by rearranging Equation 2.2:

$$\bar{L}_k = \frac{O_k \times T \times \bar{s}_k}{N_k} \left[\frac{1}{\sigma_s^2 / \bar{s}_k^2 + 1} \right] \quad (5.1)$$

Obviously, the accuracy of the MEVL is highly related to the accuracy of speed estimation. The MEVL will be used for further LT volume estimation.

5.2 LARGE TRUCK CLASSIFICATIONS

As mentioned above, whether a vehicle is a LT or not is determined by its length. Thus, in the LT volume estimation, vehicles are simply classified into two types: short vehicles (less than 12.19 m) and large trucks (greater than or equal to 12.19 m). This way of classification is different from the “Vehicle Classification Scheme F” (Wyman et al., 1985), which classifies vehicles into 15 types with 13 types explicitly defined. The classification in the “Scheme F” is based on the number of axles, axle spacing, and other features of vehicles. In the “Scheme F” that are used by most state DOTs, classes 5 to 13 are classified as trucks. Trucks of class 5 (single-unit trucks) have two axles and those of classes 6 to 13 have three axles or more.

The difference between LTs and trucks has not been explored in past studies as limited by available data. With data collected from Peek systems, we are able to discover their difference. We conducted a comparison of LTs (based on length) and trucks with three axles and up. The first dataset and lane 1 of the second dataset, described in the previous chapter, are used for the comparison. Results of the comparison are shown in Table 5.1. It is found that the percentages of LTs based on vehicle length are only slightly less than those of trucks with three or more axles based on the “Scheme F”. Therefore, The LT classification based on vehicle length in this research study is reasonable and the LT results can be used to represent all trucks excluding single unit trucks from the “Scheme F” classification method.

Table 5.1 Comparison of Truck Classification Results based on “Scheme F” and LTs

Location (lane No.)	Daily Traffic Volume (veh.)	Trucks (Based on Scheme F)		LT (Based on Length)	
		Number of Trucks (Veh.)	Percentage (%)	Number of LT (Veh.)	Percentage (%)
IH-35 in Austin (Lane 1)	27670	3289	11.89	3181	11.50
S.H.6 (Lane 1)	13037	903	6.93	816	6.26

5.3 ESTIMATION OF LT VOLUME

In the study conducted by Wang and Nihan (2001), a large sample of vehicle lengths was collected from double loop detectors and it was found that there were two peaks in the distribution of vehicle length. After separating vehicle lengths less than 12.19 m (40 ft) from the lengths greater than 12.19 m, two vehicle length distributions were obtained and each fit a normal distribution very well.

In this study, a sample of vehicle lengths from IH-35 in Austin was chosen for the study of vehicle length distribution. The Kernel density of vehicle lengths is shown in the part “a)” of Figure 5.1. The density plot displays a bimodal distribution of vehicle lengths. Small vehicle lengths are highly concentrated around 5 m and long vehicle lengths are distributed around 20 m. In order to investigate the distributions of small and long vehicles, the sample was separated into two groups, using 12.19 m as the separation point. To examine if both samples fit normal distributions, normal probability plots were utilized. Parts “b)” and “c)” of Figure 5.1 show the Q-Q plots of short and long vehicle lengths. A Q-Q plot can be used to determine if a dataset comes from a normal distribution. Obviously, the distribution of short vehicle lengths is highly right skewed and the distribution of long vehicle lengths is left skewed. The distributions of both short and long vehicle lengths are not normally distributed.

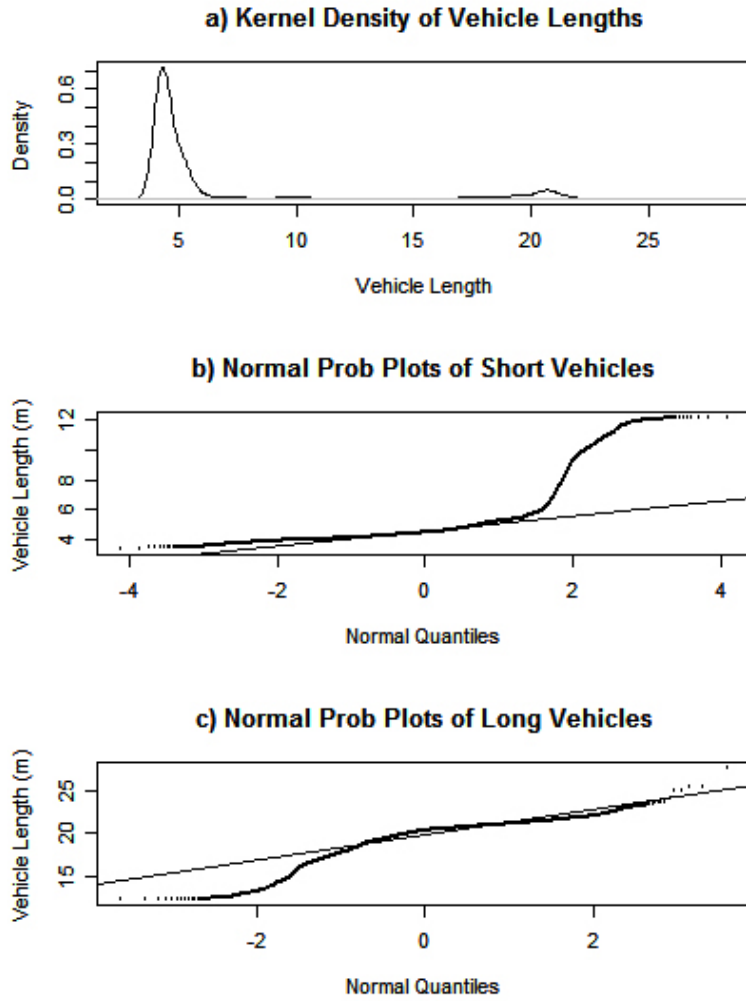


Figure 5.1 Vehicle length distributions. a) Kernel density of vehicle lengths. b) Q-Q plot of short vehicle lengths. c) Q-Q plot of long vehicle lengths.

The methodology of LT volume estimation in this study does not hinge upon the normal distribution assumptions. No matter what kind of distribution vehicle lengths fit for, we assume that the mean values of short and long vehicle lengths are l_1 and l_2 . It is also assumed that the short vehicle length distribution X and the long vehicle length distribution Y are independent. Then the average vehicle length at each time interval will be subjected to a distribution with the expectation $l = p_1 * l_1 + p_2 * l_2$, where p_1 and p_2 denote the proportions of short and long vehicles. At k th time interval, assume that N vehicle are detected, and suppose that N_1 vehicles are short vehicles and N_2 vehicles are LTs. Then, X_1, X_2, \dots, X_{N_1} form a random sample from

the distribution X , and Y_1, Y_2, \dots, Y_{N_2} form the other random sample from the distribution Y . To compute the average vehicle length (τ_i), we simply take the expectation

$$\begin{aligned}\tau_i &= E\left[\frac{X_1 + X_2 + \dots + X_{N_1} + Y_1 + Y_2 + \dots + Y_{N_2}}{N}\right] \\ &= E\left[\frac{N_1 \times l_1 + N_2 \times l_2}{N}\right] \\ &= \frac{N_1}{N} \times l_1 + \frac{N_2}{N} \times l_2\end{aligned}\tag{5.2}$$

where $N_1 + N_2 = N$, and the average vehicle length (τ_i) equals to the MEVL minus single loop length.

Two samples of historical vehicle length data from IH-35 in Austin and S.H.6 are gathered to generate vehicle length distributions of both short vehicles and LTs. Mean length (l_1) of short vehicles is around 4.88 m at SH6 and 4.72 m at IH-35; mean LT length (l_2) is about 18.96 m at SH6 and 19.39 m at IH-35. IH 35 is an urban freeway while SH6 is a rural area. The truck percentages are significantly different as shown in Table 5.1. However, u_1 and u_2 are about the same. Further investigation showed that at both locations, u_1 and u_2 for different time periods pretty much stay the same even though truck volumes and percentage may vary significantly between time periods. Therefore, u_1 and u_2 are treated as known parameters in our method and can be determined based on samples from historical vehicle length data from a similar highway in the area.

Given the MEVL value estimated and the number of vehicles at a certain time interval, the number of LTs during this time period can be calculated by:

$$N_2 = \frac{N(\tau - l_1)}{(l_2 - l_1)}\tag{5.3}$$

where l_1 and l_2 are mean short vehicle and LT lengths corresponding to a specific highway or location. Note that N_2 is rounded to the nearest integer.

5.4 APPLICATIONS

The first dataset (lane 1 data) and part of the second dataset (lane 1 data) described in the previous chapter will be used for the estimation of LT volumes. Note that the observed and estimated speeds for these two lanes are shown in Figures 4.2 and 4.3.

Using the estimated speed information, the MEVL is further estimated through Equation 5.3. Figures 5.2 and 5.3 display the observed MEVL and estimation errors. It should be noted that the estimation errors of the MEVL shown in the part “b)”s have larger values and variations during nighttime and during daytime when traffic congestion exists, indicating potential estimation accuracy issues for both time periods. The observed average vehicle lengths between midnight and 6 a.m. are generally longer than 12.19 m from the part “a)”s, a result of very high percentage of LTs in early morning hours when few passenger cars are on the road.

With speed and MEVL estimated, the LT volume at each time interval is obtained. For better illustration, LT volume data are aggregated into 1-hour intervals. Figure 5.4 shows both observed and estimated LT volumes. The estimation curves capture the observation curves very well during most hours of the day. A summary of hourly-based estimation results of LT volume for the entire day is described in Table 5.2. In this table, two Measurements of Effectiveness (MOEs) are used: the Mean Absolute Error (MAE) and Mean Absolute Percentage Error (MAPE). They are defined as

$$\begin{aligned}
 MAE &= \frac{1}{24} \sum_{i=1}^{24} \left| \hat{N}_{est.}^{(i)} - N_{obs.}^{(i)} \right| \\
 MAPE &= \frac{1}{24} \sum_{i=1}^{24} \left| \frac{\hat{N}_{est.}^{(i)} - N_{obs.}^{(i)}}{N_{obs.}^{(i)}} \right|
 \end{aligned} \tag{5.4}$$

where $\hat{N}_{est.}^{(i)}$ is the estimated LT volume during i th hour and $N_{obs.}^{(i)}$ is the observed LT volume. The overall estimated LT percentages are very close (within 0.5%) to observed percentages with slight underestimations. By comparing the estimated LT percentages with truck percentages that are computed based on vehicle classifications and shown in Table 5.2, the estimation errors are less than 1% for both datasets.

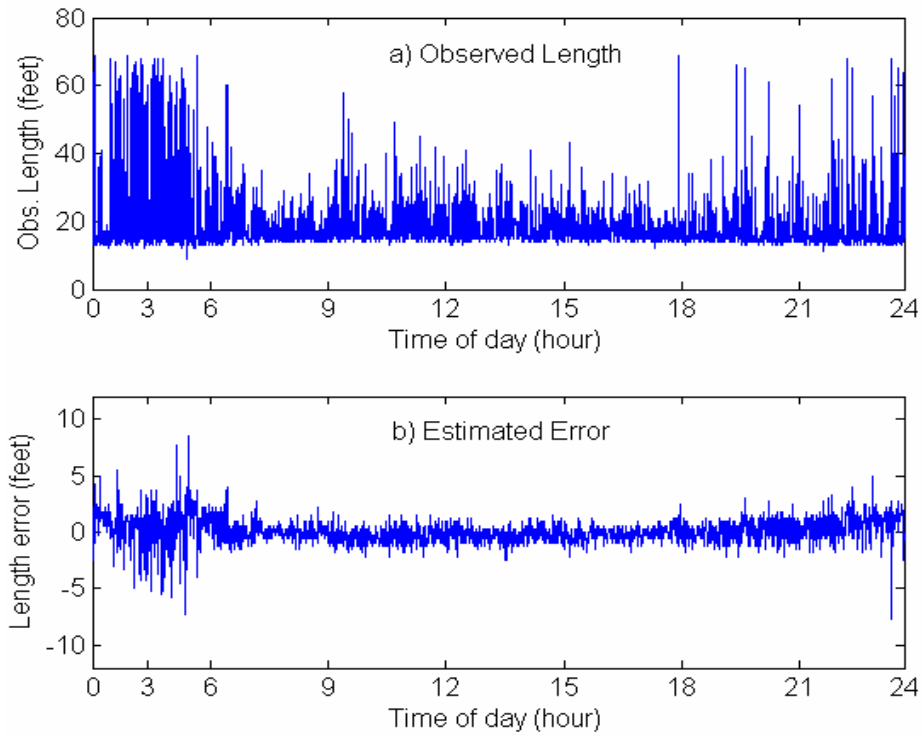


Figure 5.2 Observed MEVL and estimated errors on S.H.6 (lane 1, Jan. 27, 2004).

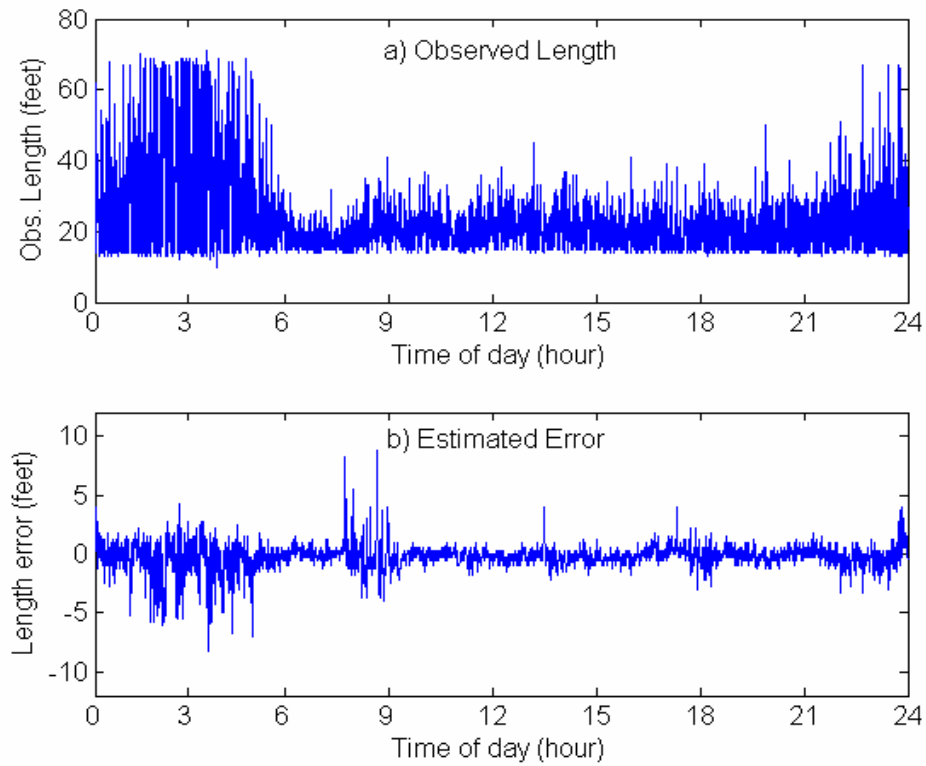


Figure 5.3 Observed MEVL and estimated errors on IH-35 (lane 1, Oct. 27, 2004).

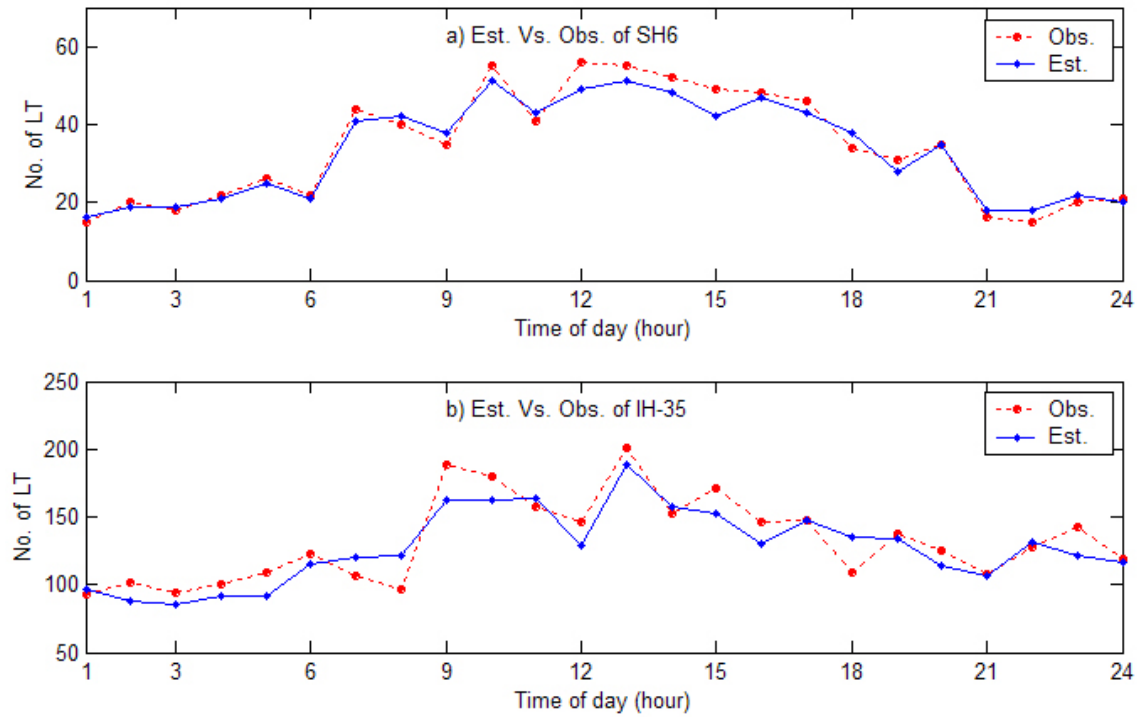


Figure 5.4 Observed and estimated LT volumes. a) Hourly-based LT volumes on S.H.6. b) Hourly-based LT volumes on IH-35.

Table 5.2 Results of hourly-based estimation of LT volume

Location (lane No.)	Traffic Volume (veh.)	Number of LT		Total LT Error (veh.)	MAE of LT (veh.)	MAPE of LT (%)
		Real (veh.)	Estimated (veh.)			
S.H.6 (lane 1)	13037	816 (6.26%)	795 (6.10%)	-21	2.54	7.57
IH-35 in Austin (lane 1)	27670	3181 (11.50%)	3064 (11.07%)	-117	11.95	9.34

To further explore the factors affecting estimation results, the effects of LT percentage and traffic volume level are investigated using the SH6 data. Firstly, a study of estimation errors under different traffic volume levels is conducted. Part “a)” of Figure 5.5 illustrates hourly traffic volumes throughout the experiment while part “c)” of this figure shows hourly Absolute Percentage Errors (APEs). Based on parts “a)” and “c)” of this figure, it is observed that APE values during nighttime when traffic volume is relatively low are generally not much smaller than those during daytime when traffic volume is relatively high, indicating that overall traffic volume does not seem to affect LT estimation accuracy. Secondly, hourly-based LT percentages are also calculated from the observed dataset and shown in the part “b)” of Figure 5.5. The LT percentages are very high between midnight and 6 a.m., and the maximum percentage is close to 40%. Nevertheless, the relative larger estimation errors in the part “c)” are not generated during those high LT percentage hours. Thus, the LT percentage itself does not show significant effects on the LT volume estimation either according to our experiment. From Figure 5.5(c), there are periods of time during the day when there are more fluctuations in APE. For example, at the 22:00 hour, the APE reaches 20%. However, a closer looking at Figure 5.4 reveals that the estimation error for the hour is only three LTs, 18 estimated versus 15 observed, and obviously acceptable. In addition, the fluctuations illustrated in Figure 6(c) are centered around the MAPE line, indicating no error trend with respect to any particular factor. This seems to indicate that the estimation results are not significantly affected by either LT percentage or overall traffic volume.

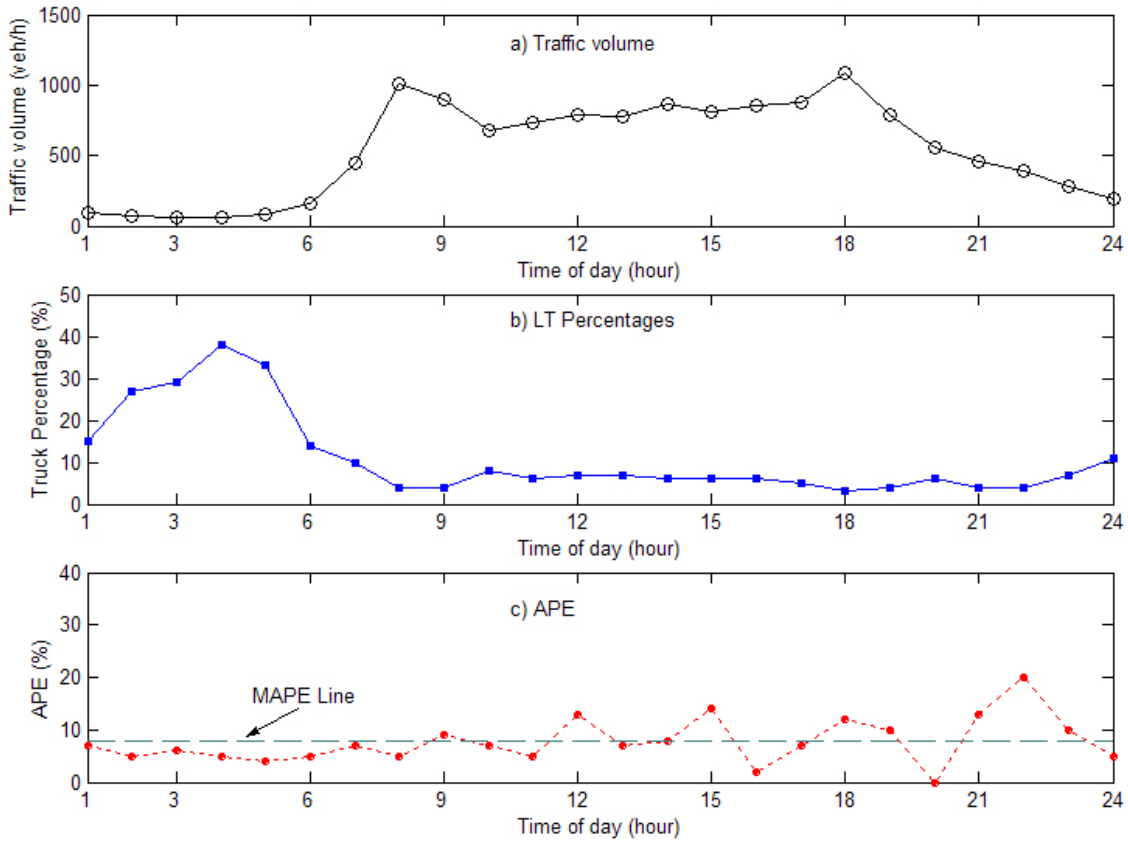


Figure 5.5 Hourly-based traffic volumes, LT percentages and estimation errors on S.H.6. a) Traffic Volume. b) LT Percentages. c) APE.

To further investigate the performance of the algorithm under various traffic conditions, particularly under congested conditions, data of two consecutive days (November 9 and 10, 2004) from IH-35 site were analyzed. The site has regular AM and PM recurrent congestion periods. Figure 5.6 presents LT estimation results along with speed estimation results and Figure 5.7 illustrate the LT estimation error distribution. For this analysis, LTs are estimated at 15-minute interval, an interval commonly used in real-time traffic flow prediction. It can be seen that again MAPE line centers around zero, indicating no systematic estimation errors. A closer look into the error distribution of the LT estimation at 15-minute interval in Figure 5.7 show that there are only 6 intervals that have error over 15 LTs per interval, or 1 LT per minute on average. About 90% of the intervals have errors smaller than 10 LTs per interval. About 80% of the intervals have errors of less than 8 LTs, or about 1 LT every 2 minutes. That's certainly good accuracy for practical applications.

From Figure 5.6, with the exception of early morning periods during which overall traffic is very light but LT percentage is very high, LT estimation accuracy did not seem to show any trend with respect to overall traffic volume, LT volume, or LT percentage. During the early morning periods (when LT% is at the highest), LT estimation accuracy is the best. The worst estimation accuracy occurred during the periods of congestion. A further investigation reveal that for the AM peak on the first day and both the AM peak and PM peak on the second day the speed estimation results are not as good as the rest of the periods. Coincidentally, those are the same three periods that have significant LT estimation errors. This indicates that traffic congestion is a factor influencing the LT volume estimation results. Traffic congestion affects speed estimation and consequently contributes to the accuracy of LT estimation.

5.5 SUMMARY

The study of the estimation of LT volume is an extension of this research project. With accurate output of speeds from the UKF, real time LT volume can be further estimated with a simple algorithm. The results show that the proposed method has good performances under various traffic conditions. Finally, the factors that influence the estimation accuracies are explored. It is found that while LT percentage and traffic volume generally do not significantly affect estimation accuracy, traffic congestion is a factor affecting the results of large truck volume estimation for the congested periods mainly due to the fact that speed estimation under congested flow conditions are typically less accurate.

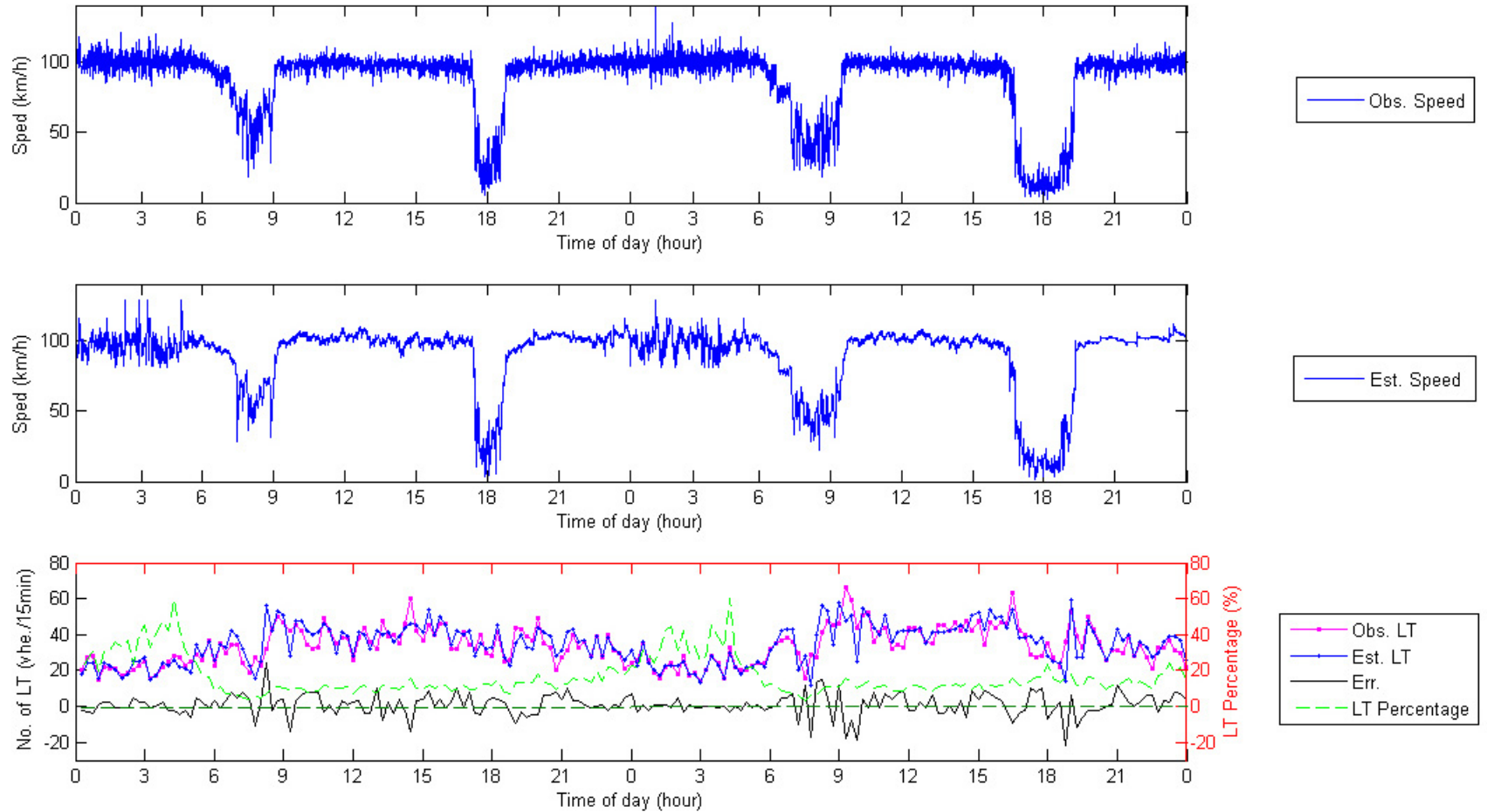


Figure 5.6 Speed and LT volume estimation results for IH-35 (Nov. 9-10, 2004).

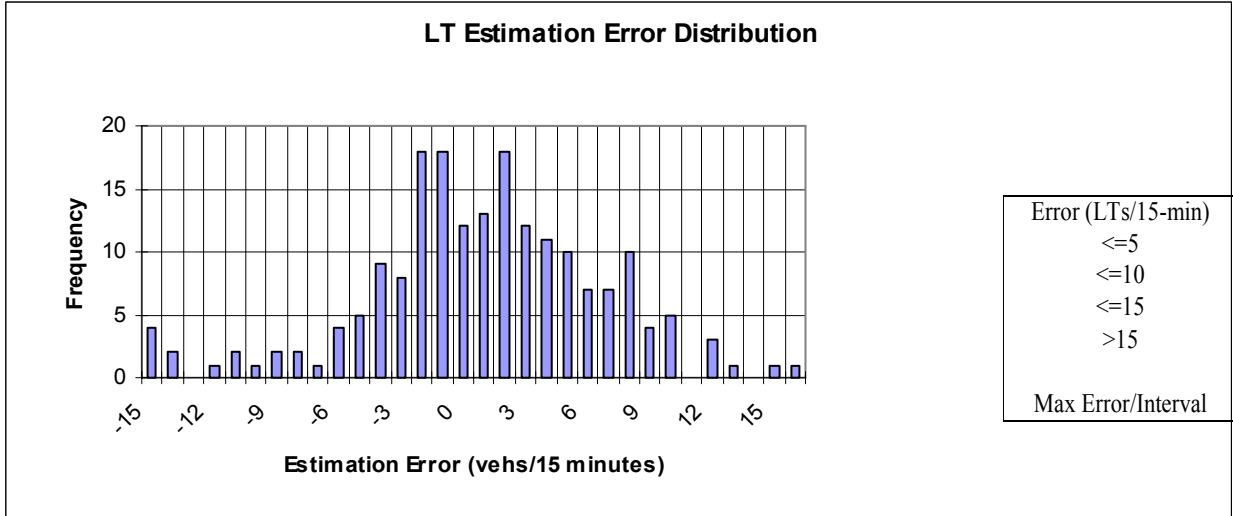


Figure 5. 7 IH-35 LT estimation error distribution (Nov. 9-10, 2004).

CHAPTER 6. SUMMARY AND CONCLUSIONS

Single loop detectors have been the most widely used detectors on the America's highways for decades. Traffic count and occupancy are typical outputs of single loop detectors. Speed estimation using single loop outputs has attracted the attention of many researchers and practitioners.

This study reviews speed estimation methods developed in past studies. Although many methods have been proposed, estimation results are still unsatisfactory due to complicated traffic conditions, the involvement of long vehicles, and limitations and simplifications in existing methods.

To achieve accurate estimation of speed, an UKF method is developed in this study. This method is suitable for solving nonlinear problems. The algorithm of the proposed method is implemented to three datasets collected from three different freeway locations. The results show that the UKF method can generate accurate and stable estimations. The UKF is also compared with EKF and g-estimator methods. The results clearly show that the UKF algorithm has superior performance. Moreover, the implementation of the proposed method is as easy as some existing methods such as the Extended Kalman Filter method.

REFERENCES

- ADR-6000 Automatic Data Recorder*. Peek Traffic Inc.
<http://www.ustraffic.net/products/data/ADR-6000-05.pdf>, accessed by September 16, 2005.
- American Association of State Highway and Transportation Officials, AASHTO. *A Policy on Geometric Design of Highways and Streets*. Washington D.C.,2001.
- Athol, P. "Interdependence of Certain Operational Characteristics within a Moving Traffic Stream." *Highway Research Record* 72, HRB, National Research Council, Washington D.C., pp 58-87, 1965.
- Bozic, S.M. *Digital and Kalman Filtering: An Introduction to Discrete-Time Filtering and Optimum Linear*. Halsted Press, New York, 1994.
- Coifman, B. "Improved Velocity Estimation Using Single Loop Detectors." *Transportation Research Part A*, Vol. 35, pp. 863-880, 2001.
- Coifman, B., and M. Cassidy. "Vehicle Reidentification and Travel Time Measurement on Congested Freeways." *Transportation Research: Part A*, Vol. 36, No.10, pp.899-917, 2002.
- Coifman, B., S. Dhoorjaty, and Z.H. Lee. "Estimating Median Velocity Instead of Mean velocity at Single Loop Detectors." *Transportation Research Part C*, Vol. 11, pp. 211-222, 2003.
- Dailey, D.J. "A Statistical Algorithm for Estimating Speed from Single Loop Volume and Occupancy Measurements." *Transportation Research Part B*, Vol. 33B, No. 5, pp. 313-322, 1999.
- Gordon, R.L., R.A. Reiss, H. Haenel, E.R. Case, R.L. French, A. Mohaddes, and R. Wolcott. *Traffic Control Systems Handbook*. FHWA-SA-95-032, Federal Highway Administration, U.S. Department of Transportation, Washington, D.C., Feb. 1996.
- Hall, F.L. "An interpretation of Speed-flow-concentration Relationships Using Catastrophe Theory." *Transportation Research Part A*, Vol.21A, No.3, pp. 191-201, 1987.
- Hall, F. and B. Persuad. "Evaluation of Speed Estimates Made with Single Detector Data from Freeway Management Systems." In *Transportation Research Record: Journal of the Transportation Research Record*, No. 1232, National Research Council, Washington, D.C., pp 9-16, 1989.
- Hazelton, M.L. "Estimating Vehicle Speed from Traffic Count and Occupancy Data." *Journal of Data Science*, 2, pp. 231-244, 2004.
- Ishimaru, J.M. and M.E., Hallenbeck. *Flow Evaluation Design Technical Report*. Washington State Transportation Center, Seattle, Washington, May 1999.

- Julier, S., and J. Uhlmann. *A general method for Approximating Nonlinear Transformations of Probability Distributions*. Oxford University: Oxford, 1996.
- Julier, S., and J. Uhlmann. "A New Extension of the Kalman Filter to Nonlinear Systems." In *International Symposium of Aerospace/Defense Sensing, Simulation, and Controls*, Orlando, FL, pp. 182-193, 1997.
- Julier, S., J. Uhlmann, and H.F. Durrant-Whyte. "A New Method for the Nonlinear Transformation of Means and Covariances in Filters and Estimators." *IEEE Transactions on Automatic Control*, Vol. 45, No. 3, pp. 477-482, March 2000.
- Kwon, J., P. Varaiya, and A. Skabardonis. "Estimation of Truck Traffic Volume from Single Loop Detector Using Lane-to-Lane Speed Correlation." Presented at *the 81st Annual Meeting of the Transportation Research Board*, Washington D.C., 2002.
- Hellinga, B. Improving Freeway Speed Estimates from Single-Loop Detectors. *Journal of Transportation Engineering*, American Society of Civil Engineers, Vol. 128, No. 1, pp. 58-67, 2002.
- Lin, W.H., J. Dahlgren, and H. Huo. "Enhancement of Vehicle Speed Estimation with Single Loop Detectors." In *Transportation Research Record: Journal of the Transportation Research Record*, No. 1870, National Research Council, Washington, D.C., pp. 147-152, 2004.
- Luz, E., Y. Mimbela, and A. Lawrence. Klein. *A Summary of Vehicle Detection and Surveillance Technologies Used in Intelligent Transportation Systems*. The Vehicle Detector Clearinghouse, New Mexico State University, 2000.
- May, A.D. *Traffic Flow Fundamentals*. Prentice Hall, ISBN 0-13-926072-2, 1990.
- McDermott, J.M. "Freeway Surveillance and Control in the Chicago Area." *Transportation Engineering Journal*, American Society of Civil Engineers, Vol.106, No.TE3, May 1980.
- Michalopoulos, P., and J., Hourdakis. "Review of Non-intrusive Advanced Sensor Devices for Advanced Traffic Management Systems and Recent Advances in Video Detection." In *Proceedings of the Institution of Mechanical Engineers*, Part I, Journal of systems and control engineering, Vol. 215, no.14, 2001.
- Nihan, N. L., X. Zhang, and Y. Wang. *Evaluation of Dual-Loop Data Accuracy Using Video Ground Truth Data*. Research Report TNW2002-02, University of Washington, January 2002.
- Oh, S., S.G. Ritchie, and C. Oh. "Real-Time Traffic Measurement from Single Loop Inductive Signatures." *Transportation Research Record 1804*, Transportation Research Board, National Research Council, Washington, D.C., pp. 98-106, 2002.

- Qgut, K.S. "An Alternative Regression Model of Speed-Occupancy Relation at the Contested Flow Level." *ARI*, the Bulletin of the Istanbul Technical University, Vol.54, No.2, 2004.
- Potter, T., (2005). *The Evolution of Inductive Loop Detector Technology*. Reno A&E, <http://www.renoae.com/Documentation/MISC/Advances%20in%20Loop%20Detector%20Technology.pdf>, accessed by Aug. 23, 2006.
- Pushkar, A., F. Hall, and J. Acha-Daza. "Estimation of Speeds from Single-Loop Freeway Flow and Occupancy Data Using Cusp Catastrophe Theory Model." *Transportation Research Record 1457*, Transportation Research Board, Washington D.C., pp.149-157, 1994.
- Rakha, H., and W. Zhang. Estimating Traffic Stream Space-Mean Speed and Reliability from Dual and Single Loop Detectors. *Transportation Research Record 1925*, TRB, National Research Council, Washington, D.C., 2005.
- Shin, E.H., and E.S. Naser. "An Unscented Kalman Filter for In-Motion Alignment of Low-Cost IMUs." *IEEE Frames Conference Proceedings*, Monterey, California, pp. 273–279, 2004.
- Sun, C., and S.G., Ritchie. "Individual Vehicle Speed Estimation Using Single Loop Inductive Waveforms." *Journal of Transportation Engineering*, American Society of Civil Engineers, Vol. 125, No. 6, Nov/Dec. 1999.
- Tom Potter. *The Evolution of Inductive Loop Detector Technology*. Reno A&E, <http://www.renoae.com/Documentation/MISC/Advances%20in%20Loop%20Detector%20Technology.pdf>, accessed by Sept. 9, 2005.
- Institute of Transportation Engineers. *Traffic Detector Handbook*. Washington D.C., 1991.
- U.S.Census Bureau. *1997 Economic Census Vehicle Inventory and Use Survey*, U.S.Census Bureau, EC97TV-US, 1998.
- U.S.Census Bureau. *2002 Economic Census Vehicle Inventory and Use Survey*, U.S.Census Bureau, EC02TV-US, 2004.
- Van der Merwe, R., E. Wan, and S. Julier. "Sigma-Point Kalman Filters for Nonlinear Estimation and Sensor-Fusion - Applications to Integrated Navigation." *AIAA Guidance, Navigation, and Control Conference and Exhibit*, Providence, Rhode Island, August 2004.
- Wan, E., and R. van der Merwe. "The Unscented Kalman Filter for Nonlinear Estimation." *Adaptive Systems for Signal Processing, Communications, and Control Symposium 2000. AS-SPCC. The IEEE 2000*, pp. 153–158, October 2000.
- Wang, Y., and N.L. Nihan. "Freeway Traffic Speed Estimation with Single Loop Outputs." In *Transportation Research Record: Journal of the Transportation Research Record*, No. 1727, pp 120-126, 2000.

- Wang, Y., and N. L. Nihan. "Dynamic Estimation of Freeway Large Truck Volume Based on Single-loop Measurements." In *the 80th Annual Meeting of Transportation Research Board*, CD-ROM, Transportation Research Board, National Research Council, Washington, D.C., 2001.
- Wyman, J. H., G.A. Braley, and R.I. Stevens. *Field Evaluation of FHWA Vehicle Classification Categories*. Rep. No. DTFH-71-80-54-ME-03, Federal Highway Administration, United States Department of Transportation, Washington, D.C., 1985.
- Yao, D., X. Gong, and Y. Zhang. A Hybrid Model for Speed Estimation Based on Single-Loop Data. In *the 7th international IEEE ITS Conference Proceedings*, MoD3.3, Washington, D.C., 2004.
- Zeeman, E. C. *Catastrophe Theory*. Addison-Wesley, Reading, MA, 1977.
- Zhang, G. , Y. Wang, and H. Wei. Artificial Neural Network Method for Vehicle Classification Using Single-Loop Outputs. In *the 85th Annual Meeting of the Transportation Research Board*, Washington D.C., 2005.